Zootaxa 4778 (3): 401–438
https://www.mapress.com/j/zt/

Article

ISSN 1175-5326 (print edition)
ZOOTAXA
ISSN 1175-5334 (online edition)

https://doi.org/10.11646/zootaxa.4778.3.1
http://zoobank.org/urn:lsid:zoobank.org:pub:01B9C95E-4CFE-4364-850B-3D994B4F2CCA

There are three species of *Chrysaora* (Scyphozoa: Discomedusae) in the Benguela upwelling ecosystem, not two

V. RAS[1,2*], S. NEETHLING[1,3], A. ENGELBRECHT[1,4], A.C. MORANDINI[5], K.M. BAYHA[6], H. SKRYPZECK[1,7] & M.J. GIBBONS[1,8]

[1]*Department of Biodiversity and Conservation Biology, University of the Western Cape, Private Bag X17, Bellville 7535, South Africa.*
[2] *verenaras@gmail.com; https://orcid.org/0000-0003-3938-7241*
[3] *simone.neethling@spu.ac.za; https://orcid.org/0000-0001-5960-9361*
[4] *adengelbrecht@uwc.ac.za; https://orcid.org/0000-0001-8846-4069*
[5]*Departamento de Zoologia, Instituto de Biociências, Universidade de São Paulo, Rua do Matão trav. 14, n. 101, São Paulo, SP, 05508-090, BRAZIL. acmorand@usp.br; https://orcid.org/0000-0003-3747-8748*
[6]*Noblis ESI, 112 Industrial Park Boulevard, Warner Robins, United States, GA 31088.*
kmbayha@gmail.com; https://orcid.org/0000-0003-1962-6452
[7]*National Marine and Information Research Centre (NatMIRC), Ministry of Fisheries and Marine Resources, P.O.Box 912, Swakopmund, Namibia. hskryp@gmail.com; https://orcid.org/0000-0002-8463-5112*
[8] *mgibbons@uwc.ac.za; http://orcid.org/0000-0002-8320-8151*
[*]*Corresponding author*

Abstract

Chrysaora (Pèron & Lesueur 1810) is the most diverse genus within Discomedusae, and 15 valid species are currently recognised, with many others not formally described. Since *Chrysaora fulgida* (Reynaud 1830) was first recognised as occurring off the south west (SW) coast off South Africa, the species has been variously synonymised with *Chrysaora hysoscella* (Linnaeus 1767) and *Chrysaora africana* (Vanhöffen 1902). Using DNA evidence alongside multivariate tools to analyse quantitative morphometric and meristic data, as well as information from the cnidome, we unambiguously separate *C. fulgida* from C. *hysoscella*; we resurrect *C. africana* as a valid species and recognise a new species, *Chrysaora agulhensis* **sp. nov.** Full descriptions of *C. fulgida*, *C. africana* and *C. agulhensis* **sp. nov.** are provided. The species have different geographical patterns of distribution around the region, with restricted areas of overlap: *C. agulhensis* **sp. nov.** is found along the southern coast of South Africa and over the Agulhas Bank, *C. fulgida* extends from Cape Point in South Africa to southern Angola, and *C. africana* can be found from southern Namibia northwards to the Gulf of Guinea. The species can be readily separated in the field by a combination of tentacle/lappet number and shape, colour patterns and the form of the oral arms.

Key words: Agulhas Bank, Benguela upwelling region, Namibia, New species, Pelagiidae, Scyphozoa, Taxonomy

Introduction

The genus *Chrysaora* is considered the most speciose genus within the subclass Discomedusae (https://www.marinespecies.org/) and comprises 15 valid species (Morandini & Marques 2010; Bayha *et al.* 2017), with a number of others recognised but not formally described, or redescribed (Bayha *et al.* 2017; Gómez-Daglio & Dawson 2017). The genus is widely distributed throughout coastal oceans (Morandini & Marques 2010), and contains some very abundant and ecologically important members that can influence ecosystem functioning and trophic flows. For example, they are unselective predators and can collapse food chains when populations explode (Feigenbaum & Kelly 1984; Suchman *et al.* 2008; Lucas *et al.* 2012; Brodeur *et al.* 2016; Bologna *et al.* 2018).

Until the recent study of Bayha *et al.* (2017), six species of *Chrysaora* were recognised in the Atlantic Ocean (Morandini & Marques 2010): *C. hysoscella* (Linnaeus 1767) in the temperate north eastern (NE) Atlantic and Mediterranean Sea, *C. quinquecirrha* (Desor 1848) in the temperate north western (NW) Atlantic, *C. lactea* (Eschscholtz 1829) in the tropical and warm temperate waters of the eastern (E) Atlantic (Caribbean Sea to central Argentina), *C.*

Accepted by M. Dawson: 31 Mar. 2020; published: 15 May 2020

plocamia (Lesson 1830) in the cold temperate and polar waters of the south western (SW) Atlantic and south eastern (SE) Pacific and *C. fulgida* (Reynaud 1830) in the temperate and tropical waters off western (W) Africa. Few of these species have been observed in sympatry (Morandini & Marques 2010; Gómez-Daglio & Dawson 2017).

The recent results of Bayha *et al.* (2017) add a further two species to the Atlantic fauna, both of which overlap in their geographic distribution with congenerics but, differ in their degree of ecological overlap. *Chyrsaora chesapeakei* (Papenfuss 1936) occurs in the estuarine waters of the NW Atlantic and coastal waters off the Gulf of Mexico and, was split from *C. quinquecirrha* using genetics along with various morphological and morphometric measures (Bayha *et al.* 2017). Although these species overlap in their geographic distributions it must be noted that *C. chesapeakei* appears to be a largely estuarine species while *C. quinquecirrha* is predominantly coastal, with limited areas of overlap between the two (Bayha *et al.* 2017). Bayha *et al.* (2017) also distinguished *C. africana* (Vanhöffen 1902), which occurs along the W and SW coasts of Africa, from *C. fulgida* which only occurs along the SW coast of Africa, on the basis of differences in DNA. *Chrysaora africana* and *C. fulgida* are both coastal species and are regularly observed in sympatry off the coast of northern Namibia (Neethling 2010).

Recent work by Abboud *et al.* (2018) has shown that significant genetic structuring within described species, exists at a variety of levels, from typical intraspecific variation to the existence of cryptic species within some Large Marine Ecosystems (LMEs). Although data from the Benguela Current LME (BCLME) were not included in the analyses of Abboud *et al.* (2018), Bayha *et al.* (2017) showed that this structuring is also evident in the BCLME with their separation of *Chrysaora africana* and *C. fulgida*. Interestingly, distinctions within LME structure can be observed in some "species" at geodesic distances of less than 50 km (Abboud *et al.* 2018). It is therefore not unlikely that such structure would also be observed within LMEs that span an environmental range or contain potential environmental barriers to consistent gene flow. It is only by adding to our knowledge of species diversity within these systems that we can begin to draw phylogeographic patterns and clarify whether these patterns are driven environmentally, regionally, taxonomically, or functionally (Abboud *et al.* 2018).

The BCLME is a heterogeneous and variable system that may drive genetic heterogeneity. The environments in the extreme north (S Angola–17.28°S) and south (Agulhas Bank— ~37°S) are quite different, influenced at these latitudinal limits by subtropical waters of the Angola and Agulhas currents, respectively (Hutchings *et al.* 2009). The northern Benguela upwelling area is defined as the region north of the Lüderitz upwelling cell at ~26°S and, is characterised by a relatively broad shelf and a sluggish circulation: it supports a high phytoplankton biomass and (consequently) experiences routine hypoxia in parts (Hutchings *et al.* 2009). By contrast, the southern Benguela upwelling ecosystem is more hydrodynamically active and it displays a pronounced seasonality in, and often intense, coastal upwelling. Whilst the continental shelf along the west coast of South Africa itself is relatively narrow, it extends offshore of Cape Agulhas in the south to a distance of 250 km and, narrows progressively eastwards to Port Elizabeth. This region is known as the Agulhas Bank and it is subject to shelf-edge upwelling, and coastal upwelling at isolated capes and peninsulas (Hutchings *et al.* 2009). It is an area of strong seasonality in environmental productivity, but comparatively sluggish circulation (Hutchings *et al.* 2009).

Chrysaora fulgida was described from Type material collected off the Cape of Good Hope (Reynaud 1830). It was subsequently recorded north of that point, all the way along the west coast of South Africa and Namibia (Kramp 1961; Morandini & Marques 2010; Neethling 2010; Sink *et al.* 2017). In 1902, however, Vanhöffen caught two damaged specimens of *Chrysaora* from Algoa Bay along the south coast of South Africa. Although he recognised these as distinct from *C. africana*, and he tentatively considered they might be *C. fulgida,* he described them as *Chrysaora* sp. Algoa Bay is situated 790 km from the Cape of Good Hope, and the environment in this part of the Agulhas Bank is quite different from that of the Type locality. Technically, it falls within the Agulhas Current LME (ACLME) (Lutjeharms & Cooper 1996; Vousden *et al.* 2012), and it is characterised by warm, fast flowing waters. It is considered quite unstable and exhibits meanders as well as shear eddies and plumes, with the eastern corner characterised by a persistent upwelling shell (Vousden *et al.* 2012). These specimens were described as possessing pale spots on the exumbrella surface (Vanhöffen 1902); a qualitative feature not included in any descriptions of *C. fulgida*. A number of specimens of a species of *Chrysaora* bearing white exumbrella spots have been collected along the length of the south coast of South Africa recently. In order to examine the taxonomy of *Chrysaora* off Southern Africa, we took genetic (mitochondrial cytochrome *c* oxidase subunit I, ribosomal 18S, nuclear internal transcribed spacer I and II as well as ribosomal 5.8S), macromorphological and cnidome data from specimens collected from Angola to South Africa. Our analysis comprehensively separate *C. fulgida* and *C. africana*, while revealing the presence of the novel species, *C. agulhensis* **sp. nov**. In addition, we provide formal, updated descriptions of each.

Materials and methods

Sample Collection and Material Examined

Specimens of medusae of *Chrysaora* in good condition were collected from between northern Namibia and the Agulhas Bank off South Africa, over the period January 2003–December 2018. In addition to using beach-stranded material, pelagic and demersal trawls, MOCNESS plankton, and surface dip-nets were also used to collect specimens at sea. Full details of all samples collected and analysed here are provided in Table 1 and in the relevant descriptions. Upon collection, a small piece of oral arm tissue was removed from each specimen for genetic analysis, before the balance of the individual was preserved in 5% formalin in ambient seawater. The material collected for genetic analyses was stored in 96–100% ethanol at -20°C until analysed. Comparative morphological material for *C. hysoscella* was obtained from the collections at the Natural History Museum (NHM), London (Table 1).

TABLE 1. Full details of specimens analysed throughout this study (2003-2015) (medusae only), including *Chrysaora hysoscella* specimens analysed at the National History Museum, London (NHM). Table also indicates species and localities from which genetic material (indicated by *) was extracted and larvae were settled (indicated by **).

Species	Collection Date	N	Collection Locality	Coordinates	Museum Catalogue/ Accession
C. hysoscella	-	2	Haven Cove Creek, Kent	38.86°N,76.3°W	25.8.11.1
C. hysoscella	-	1	Leigh Creek	-	26.3.10.21
C. hysoscella	-	1	On a beach, Sea View	51.39°N,1.37°E	1934.8.20.1
C. hysoscella	-	7	Sula Plymouth Laboratory	50.39°N,4.14°W	1982.11.30.276
C. hysoscella	-	1	Margate, Kent	51.38°N,1.24°E	1983.8.5.1
C. hysoscella	-	1	Salcombe, Devon	50.24°N,-3.78°W	98.5.7.2
C. africana	01.03.2008–30.04.2008	16	Namibia*	23.33˚S, 14.2˚E–23.67˚S, 13.25˚E	SAMC H5155
C. africana	12.5.2014	5	West Coast, South Africa*	34.10˚S, 18.48˚E	-
C. africana	10.10.1898	4	Fish Bay, Angola	16.55˚S,11.77˚E	ZMB CNI 5949
C. africana	8.1938	2	Walvis Bay, Namibia	22.95°S,14.48°E	NNM 5361, ZMA 2019
C. africana	18.12.1959	7	Gulf of Guinea, Togo	2.85°N,3.17°W	USNM 53871
C. africana	29.08.1963	7	Point Noire, Congo	4.79°S,11.81°E	ZMH C7452, ZMH C7451
C. fulgida	01.03.2008–30.04.2008	40	Namibia**	23.33˚S, 14.2˚E–23.67˚S, 13.25˚E	SAMC H5156
C. fulgida	5.6.2013	8	Southern Coast, South Africa**	33.82°S,22.47°E	-
C. hysoscella	2009	3	Ireland*	53.39°N,10.19°W	-
C. agulhensis **sp. nov.**	12.4.2014	11	Muizenberg, South Africa*	34.11˚S, 18.37˚E	MB-A088458
C. agulhensis **sp. nov.**	13.10.2014	4	Gouritzmond, South Africa*	34.35˚S, 21.89˚E	-
C. agulhensis **sp. nov.**	15.03.2011	10	Zewenwacht, South Africa	34.11˚S, 18.79˚E	-
C. agulhensis **sp. nov.**	12.11.2012	4	False Bay, South Africa**	34.13˚S, 18.44˚E -34.10˚S, 18.48˚E	-

Ephyrae were either collected *in situ* or following the laboratory rearing of polyps. *In situ* material of *C. fulgida* was collected off Walvis Bay using a small plankton net fitted with a 200 µm mesh; specimens were examined live in the laboratory prior to subsequent preservation in 5% seawater formalin. For laboratory-reared material, sperm and eggs from mature specimens were released into ambient seawater, and following fertilization, planulae were collected and settled following the protocols of Widmer (2005). Polyps were then reared in the laboratory until strobilation, and ephyrae cultured. Polyps and ephyrae were examined live prior to subsequent preservation in 5% formalin.

Morphological and meristic data

Preservation often results in weight loss and shrinkage (Lucas 2009) and Thibault-Botha & Bowen (2004) suggest these effects are pronounced in gelatinous zooplankton due to their high water content. These effects often vary with organism size and period of preservation (de Lafontaine & Legget 1989) but de Lafontaine & Legget (1989) suggest these effects stabilise after a minimum of 60 days in preservation. The present study did not correct for any preservation effects as all measurements were taken approximately 90 days after fixation.

Following the protocols of Morandini & Marques (2010), a number of morphometric and meristic features were measured and determined from entire and dissected specimens; these are summarized in Table 2. All measurements (to the nearest 0.5 mm) were taken using vernier callipers, under either a magnifying glass or a dissecting microscope at various magnifications. Descriptions of ephyrae broadly follow those of Straehler-Pohl & Jarms (2010).

TABLE 2. List of the morphological features measured (mm) or counted on the *Chrysaora* specimens examined, and the codes assigned to each, modified from Morandini and Marques (2010).

Morphological feature number (MF)	Morphological feature description	MF	Morphological feature description
S 1	Umbrella diameter	S 20	Length of ostia
S 2	Maximum umbrella height	S 21	Number of oral arms
S 3	Minimum umbrella height	S 22	Length of intact oral arm
S 4	Number of octants	S 23	Width of oral arm originating from umbrella
S 5	Number of velar lappets in octant	S 24	Maximum width of oral arm
S 6	Velar lappet length	S 25	Difference in length from (S 22) to (S 23)
S 7	Velar lappet width	S 26	Maximum frill width
S 8	Rhopalial lappet length	S 27	Minimum frill width
S 9	Rhopalial lappet width	S 28	Number of primary tentacles
S 10	Tertiary lappet width‡	S 29	Number of primary tentacles base stalks
S 11	Tertiary lappet length‡	S 30	Width of primary tentacle base
S 12	Number of gastrovascular pouches	S 31	Number of secondary tentacles
S 13	Width of oral opening pillar	S 32	Width of secondary tentacle base
S 14	Diameter of oral opening	S 33	Number of tertiary tentacles‡
S 15	Manubrium length	S 34	Width of tertiary tentacle base‡
S 16	Manubrium depth	S 35	Number of rhopalia
S 17	Number of ostia	S 36	Gonad width
S 18	Inter-ostia width	S 37	Gonad length

Morphological measures often vary with animal size (McClain *et al.* 2015) and although it is customary to account for this in any comparisons between species using ANCOVA (Miller & Chapman 2001), our study did not have a wide enough size range or consistency in the size ranges between species. ANCOVA also typically does not allow for comparisons between multiple variables across species. Morphological features that change with animal size may do so in a fixed (isometric) or size-dependent (allometric) manner. Without access to a wide range of size classes in comparative studies, it is more appropriate to focus on identifying distinctive isometric than allometric features, because of unknowns that may influence the precise nature of allometric relationships in different environments. To counteract this size-bias, measures were first standardized by dividing all by bell diameter and $\log_{10}$ transformed. Correlations (Pearson's R, or Spearman's Rank, normality- and homoscedacity-dependent: Zar 1999) were then performed between all standardized measures and bell diameter, and allometric features were dropped from inclusion in the multivariate analyses (see below).To examine the multivariate dissimilarity between the *Chrysaora* studied, we used the Canonical Analysis of Principal Coordinates (CAP) routine in PRIMER 7 & PERMANOVA+. The CAP routine seeks a set of axes that best discriminates amongst previously defined groups (the three putative species and *C. hysoscella* from the NE Atlantic) in a multivariate space (Anderson *et al.* 2008), and is akin to a non-parametric discriminant functions analysis. The initial series of orthonormal principle coordinates (PCO) was generated from a character resemblance matrix between specimens, based on Euclidean distance. It is important

to note that the Euclidean distance matrix between specimens was based on those standardised measures that were common to all specimens, and that were size-independent. Conventionally, in a canonical discriminant analysis, a subset of PCO axes are chosen manually, based on the number of variables in the original data matrix. However, in the present study we followed Anderson *et al.* (2008) and have used the "*leave-one-out*" diagnostics to determine the subset of PCO axes. Using a matrix based on the different species that is generated in parallel by the software routine, a classical canonical analysis is then computed with the identified subset of PCO axes to provide canonical eigenvalues and their associated eigenvectors, which can be used to produce a CAP plot. These CAP axes, which are linear combinations of a subset of orthonormal PCO axes, were also used to cross validate specimen identity and determine misclassification errors. In order to determine which morphological variables characterised the differences between species, we have superimposed vectors corresponding to Spearman rank correlations with the CAP axes: only those variables with Spearman rank correlations > 0.55 have been illustrated.

Cnidome

Tissue for analyses were prepared as described in Peach & Pitt (2005), for five specimens of each of *Chrysaora fulgida*, *C. africana* and the southern coast material. In the case of regionally collected material, samples were dissected from the tentacles and oral arms of preserved specimens because it has been suggested that the abundances of various nematocysts between each varies (Peach & Pitt 2005). Undischarged nematocysts were isolated by placing the tissue in a 10% solution of Sodium Thyocyanate (Mariottini *et al.* 2008), then homogenized using a mortar and pestle, squashed beneath a microscope cover-slip and examined, unstained, at 1000 × magnification. Discharged nematocysts were obtained in a trial-and-error manner utilising a number of techniques: 1) by placing tissue samples in a (60%) saline solution and then passing a 20 mA current through it using a wire connected to a 12V battery, prior to squashing; 2) hydrating the tissue in distilled water for 3, 5, 8 or 10 days (Mejía-Sánchez & Marques 2013) before squashing; and/or 3) allowing the tissue on the slide to dry slightly before squashing. In some cases, discharge was simply not possible.

Under the microscope, nematocysts were identified following Mariscal (1974) and Östman (2000). The relative abundance of each type of nematocyst in each tissue sample was determined from counts in 10 random fields of view. The maximum width and length of the capsule and, length of the tubule, of at least ten discharged and undischarged nematocysts for each identified type were measured from each tissue sample using a graticule. Note: the cnidome of *C. hysoscella* from the NE Atlantic was not investigated directly here.

In order to determine whether the relative abundance of each nematocyst type differed between tissue types and taxa, Chi-square tests (Zar 1999) were performed using SPSS 22 Ltd., for the null hypothesis of no dissimilarities. Tests between tissues were computed within taxa, whilst tests between taxa were computed separately by tissue type.

Nematocyst measures (capsule width and length, and shaft length) were $\log_{10}$ transformed, and tested for normality and homoscedasticity, before a two-way ANOVA (Zar 1999) was used to compare sizes across species and tissue. Undischarged and discharged nematocysts were analysed separately. Post hoc tests were performed where measures were statistically different. The Bonferroni procedure was applied to all statistics in order to control for Type I errors (Quinn & Keough 2002).

DNA Analysis

DNA extraction, amplification and sequencing

Total genomic DNA extractions, precipitations and quantifications were performed following a standard phenol-chloroform extraction (Wallace 1987; Sambrook & Russell 2001; Neethling 2010). The Cytochrome *c* oxidase subunit I (COI) region was amplified using the primers listed in Table 3. A maximum of 620 base pairs were amplified from 17 samples for the COI gene region using a ramp up cycle with reaction conditions: 94˚C for 8 min; then one cycle of 54.2˚C for 2 min, 72˚C for 2 min, 94˚C for 4 min; followed by one cycle of 55.2˚C for 2 min, 72˚C for 2 min, 94˚C for 45 sec; followed by 33 cycles of 56.2˚C for 45 sec, 72˚C for 1 min, followed by a final step of 72˚C for 5 min before storage at 4˚C. The 18S region was amplified as a single amplicon using the primers listed in Table 3 and a maximum of 1800 base pairs was amplified from 14 samples with reaction conditions: 95˚C for 5 min; followed by 37 cycles of: 93˚C for 1 min, 48˚C for 1 min, 72˚C for 2 min, followed by a final step of 72˚C for 10 min

before storage at 4˚C. The ITS1, ITS2 and 5.8S gene regions were all amplified using the ITS primers listed in Table 3 and a maximum of 752 base pairs were amplified from 14 samples with reaction conditions: 94˚C for 8 min, 49˚C for 2 min, 72˚C for 2 mins followed by; 94˚C for 4 min, 50˚C for 2 min, 72˚C for 2 mins; followed by 33 cycles of 94˚C for 45s, 51˚C for 45s, 72˚C for 1 min; followed by a final step of 72˚C for 5 min before storage at 4˚C. All PCR reactions were carried out using 25 μL reaction volumes on a Techne ® endurance TC-512 gradient thermal cycler (Barloworld Scientific). Two micro litres of the PCR product was visualized on a 7% agarose gel, following which the remainder was then purified with a nucleoFast 96 PCR kit (Macherer-Nagel). Using BigDye chemistry, the cleaned products were then cycle sequenced and analysed with an ABI 3730 XL DNA Analyzer (Applied 514 Biosystems Inc.) at the Central Analytical Facility (University of Stellenbosch). In some cases, amplification was just not possible despite repeated attempts.

TABLE 3. PCR primers used to amplify the cytochrome *c* oxidase subunit I (COI), 18S ribosomal and the nuclear ITS gene regions in this study.

Region	Primer Name	Sequence (5'-3')	Reference
COI	LCOjf	GGTCAACAAATCATAAAGATATTGGAAC	Dawson 2005a
	AaCOIi-L	GCCCGTYYTAATAGGRGGGTTTG	Dawson and Jacobs 2001
	KMBMT-71	TGGTGCTTTTTCAGCTATGATTGG	Bayha 2005
	HCOCato	CTCCAGCAGGATCAAAGAAG	Dawson 2005a
	HCO2198	TAAACTTCAGGGTGACCAAAAAATCA	Folmer *et al.* 1994
ITS	jfITS1-5f	GGTTTCGTAGGTGAACCTGCGGAAGGATC	Dawson and Jacobs 2001
	jfITS1-3r	CGCACGAGCCGAGTGATCCACCTTAGAAG	Dawson and Jacobs 2001
18S	18Sa	AACCTGGTTGATCCTGCCAGT	Medlin *et al.* 1988
	18Sb	GATCCTTCTGCAGGTTCACCTAC	Medlin *et al.* 1988

Sequence processing

All sequences were processed using Geneious v.11.1.4 (http://www.geneious.com/). Firstly, misreads within sequences were corrected and poorly determined terminal portions discarded. Sequences were then compared to the GenBank nucleotide database via BLASTn (Altschul *et al.* 1997) to confirm the correct region had been sequenced. Contigs were then assembled using the ClustalW alignment tool within Geneious. 18S contigs typically had overlapping regions of roughly 500–650 bp and where the overlapping portions were highly ambiguous, sequences were discarded. COI sequences were then translated into protein sequences and verified on GenBank using Blastp. A reference sequence of *C. pacifica* (GenBank accession no.: KY610838.1) was used to identify, map and extract individual ITS gene regions from contigs for analyses. GenBank accession numbers for our study can be found in Appendix 1.

Phylogenetic and evolutionary analyses

Mean pairwise sequence differences using uncorrected "*P*", and maximum parsimony trees were calculated in PAUP v.10.4b (Swofford 2003), for COI, 18S, ITS1, ITS2 and 5.8S (data for 5.8S not shown) sequences. The maximum parsimony tree infers hypothetical evolutionary phylogenetic relationships between species. The tree was calculated by performing a heuristic parsimony, using a branch swapping algorithm, also known as the tree-bisection-reconnection method, with all characters assigned an equal weight and left unordered. A bootstrap procedure was then performed in order to test the stability of the nodes, using 1 000 resampling replicates and the tree-bisection-reconnection method. Only bootstrap values above 75% were considered well supported and retained in the final tree (Felsentein 1985). It has been shown by various studies (e.g. Ogden & Rosenberg 2007; Dwivedi & Gadagkar 2009) that gap treatment does not necessarily significantly affect the accuracy of analyses where the gap percentage within a particular dataset is <20% as was the case for our datasets. We therefore treated gaps as missing/ambiguous in all analyses.

The Akaike information criterion was used in the programme JModeltest v.2.1.2 (Darriba *et al.* 2012) in order to determine the "best fit model of evolution" for the COI (TPMuf+I+G), 18S (GTR+I+G), ITS1 (TIM2+I+G) and ITS2 (TIM2+G) gene fragments (Akaike 1973; Nylander 2004). Bayesian analyses were then performed in Mr. Bayes v.3.2 (Ronquist & Hulsenbeck 2003), using this model as a guide and included five Monte Carlo Markov

chains. The resultant chains were sampled every 1 000th generation and a total of 10 million generations were used. In order to determine statistical stationarity, the "sump" command in Mr. Bayes was used to summarize the generated samples. Based on these results, 25% were discarded as burn-in. To assess whether the data were adequately sampled, the potential scale reduction factor was determined (PSRF) (Ramhaut & Drummond 2007). Following this the "sumt" command was executed in Mr. Bayes in order to summarize trees. These trees were then visualized using the programme Figtree v.1.4.2 (http://tree.bio.edu.ac.uk/software/gtree) and those nodes with posterior probabilities $p < 0.95$ were considered not significantly supported. All analyses performed above were repeated for a concatenated dataset of the 18S, ITS1, ITS2 and 5.8S (evolutionary model = GTR+I+G), when all regions could be amplified for the same individual.

A Maximum Likelihood analysis was also performed on individual gene regions as well as the concatenated nuclear dataset using the best model of evolution determined previously (Darriba *et al.* 2012). The bootstrap consensus tree was inferred from 10 000 permutations (Felsentein 1985) and was taken to represent the evolutionary history of the taxa analysed (Felsentein 1985). Branches corresponding to partitions reproduced in less than 50% bootstrap replicates were collapsed. Initial tree(s) for the heuristic search were obtained automatically by applying Neighbor-Join and BioNJ algorithms to a matrix of pairwise distances estimated using the Maximum Composite Likelihood (MCL) approach, and then selecting the topology with superior log likelihood value. All positions containing gaps and missing data were eliminated. Evolutionary analyses were conducted in MEGA X (Kumar *et al.* 2018).

A calibrated timetree was then generated using the RelTime method (Nei & Kumar 2000) for the concatenated nuclear dataset. The RelTime method was chosen because it is a fast-dating and high-performance algorithm that can be implemented directly in MEGA X (Mello 2018). It enables the estimation of relative divergence times without the need for a pre-specification of the statistical distribution of lineage rates, making it orders of magnitude faster than traditional Bayesian methods (Tamura *et al.* 2012). Thus, using the Maximum Likelihood method described previously, divergence times for all branching points in the topology were calculated. Calibration of the molecular clock was performed based on estimates obtained from Gómez-Daglio (2016; Chapter 3) with the upper limit set to 15 Mya and the lower limit set to 25 Mya. The original tree was drawn to scale (not shown), with branch lengths measured in the relative number of substitutions per site. All positions containing gaps and missing data were eliminated. This analysis was used as a preliminary investigation into the possible divergence times of these taxa however more robust analyses including a larger number of taxa may be required to improve the resolution of times.

Lastly, a range of diversity and gene flow measures were calculated using DNAsp v6.11.01. Using the "Genetic Diversity Analysis" the following measures were computed: number of haplotypes, "*h*"; haplotype diversity, "Hd" (Nei 1987, equation 8.4); average number of nucleotide differences, "K" (Tajima 1983, equation A3); nucleotide diversity with the Jukes and Cantor correction, "Pi(JC)" (Lynch and Crease 1990, equations 1-2) and the average number of nucleotide substitutions per site between taxa, "Dxy" (Nei 1987, equation 10.20).

Results

Morphological and meristic data

A total of 16 standardized measures were uncorrelated with individual size (Table 4), of which four were common to all specimens (Table 4). The CAP plot (Fig. 1) shows that two axes are needed to distinguish between the recognised species (i.e. *Chrysaora fulgida*, *C. hysoscella* and *C. africana*) and the south coast specimens of *Chrysaora* examined here, and the canonical correlations associated with each eigenvalue are large ($\delta_1^2 = 0.97$, $\delta_2^2 = 0.92$). The *leave-one-out* procedure resulted in a total of eight orthonormal PCO axes being used in the final CAP analysis, and 96.21% of all specimens were correctly assigned to their respective putative taxon: with one *C. fulgida* being incorrectly assigned to *C. hysoscella* from the NE Atlantic and one of the south coast specimens being assigned to *C. fulgida*. The first CAP axis separates out *C. africana* from the balance of taxa, whilst the second, to the right, separates *C. fulgida/C. hysoscella* from the south coast specimens (Fig. 1).

TABLE 4. Summary of the standardized measures (% maximum bell diameter) from all the specimens of *Chrysaora fulgida, C. africana* and *C. agulhensis* **sp. nov.** examined here. Data as mean measure, number of specimens examined, and standard deviation. Also shown are the significant (* $p < 0.05$, adjusted for multiple testing) correlation coefficients between $\log_{10}$ transformed raw measures and individual size: P, Pearson's R; S, Spearman Rank. Standardized measures that are significantly size-dependent indicated in bold. The final two columns indicate the significance (* $p < 0.05$, adjusted for multiple testing) test statistics (t statistic (t) from student's t-test; Z statistic (U) from Mann-Whitney U test) generated from comparisons of the means of $\log_{10}$ transformed standardized measures between taxa (*Cf, C. fulgida; Ch, C. hysoscella; Ca, C. africana*): n/s, not significant ($p > 0.05$). See Table 3 for key to character codes. ‡, standardized morphological measures used in CAP analysis.

	Chrysaora fulgida				***Chrysaora agulhensis* sp. nov.**				***Chrysaora africana***				***C. fulgida* vs. *C. agulhensis* sp. nov.**	***C. africana* vs. *C. agulhensis* sp. nov.**
MF	Mean	StD	N	Corr	Mean	StD	N	Corr	Mean	St. Dev.	N	Corr	*p*	*p*
S 2 ‡	0.18	0.86	40	n/s	-1.03	0.31	30	0.23*(P)	0.06	0.02	16	n/s	_3.5*(t)	_3.5*(t)
S 7 ‡	0.08	0.01	18	0.90*(S)	-1.01	0.57	29	n/s	0.03	0.01	16	n/s	_3.64*(t)	_7.76*(t)
S 9 ‡	0.07	0	18	0.90*(S)	-1.14	0.23	30	n/s	0.03	0.01	16	n/s	_8.78*(t)	_4.04*(t)
S 10	-	-	-	-	-1.23	0.23	30	n/s	0.05	0.01	16	0.86*(P)	-	-
S 14	**0.18**	0.03	40	0.79*(S)	**-0.9**	0.28	24	0.05*(P)	0.28	0.04	16	0.84*(S)	_6.6*(t)	6.06*(t)
S 15 ‡	0.36	0.03	39	0.99*(P)	-0.72	0.26	24	n/s	0.33	0.05	16	0.96*(P)	_3.26*(Z)	_3.26(Z)
S 16 ‡	0.004	0.00	32	0.88*(P)	**-0.87**	0.31	24	0.38*(P)	0.01	0	16	n/s	_18.2*(t)	_4.04*(Z)
S 18	0.09	0.01	39	0.96*(P)	-0.78	0.23	25	n/s	**0.07**	0.02	16	n/s	_10.65*(t)	_10.32*(t)
S 19	**0.06**	0.02	40	n/s	-1.21	0.25	26	n/s	0.15	0.02	16	0.83*(S)	9.57*(t)	n/s
S 20	**0.1**	0.03	40	n/s	**-1.01**	0.28	26	0.3*(P)	0.13	0.03	16	n/s	2.38*(t)	n/s
S 22	1.68	0.34	29	0.78*(S)	0.1	0.26	8	n/s	**2.97**	0.93	5	0.99*(S)	6.6*(t)	n/s
S 23 ‡	0.21	0.05	40	n/s	**-0.87**	0.29	19	0.22*(P)	0.21	0.08	15	n/s	n/s	n/s
S 24 ‡	0.41	0.05	40	0.97*(P)	**-0.39**	0.31	10	0.35*(P)	0.52	0.13	14	0.86*(P)	n/s	n/s
S 30	0.02	0	5	0.90*(S)	-1.67	0.27	29	0.07*(P)	**0.02**	0	12	n/s	_3.03*(t)	3.73*(t)
S 32	0.01	0	5	n/s	-1.74	0.27	29	0.08*(P)	0.01	0	12	n/s	_3.05*(Z)	4.37*(Z)

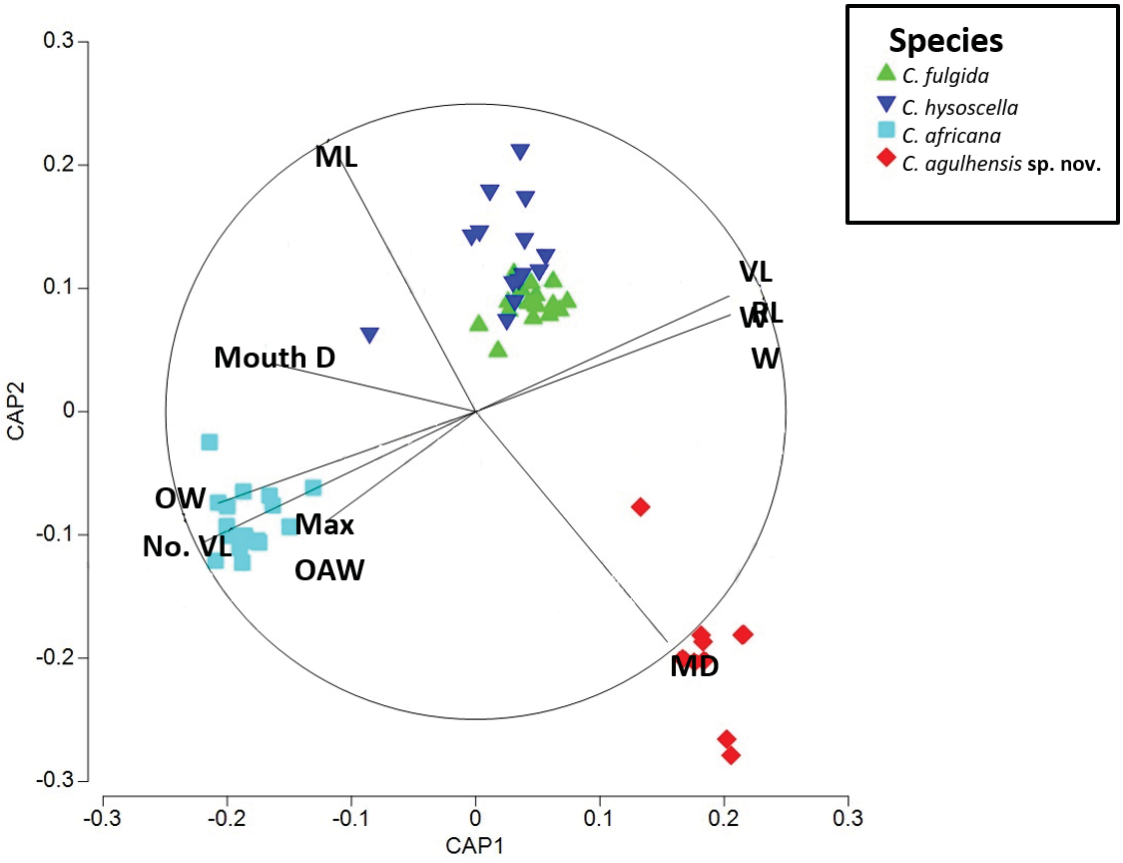

FIGURE 1. Canonical ordination plot of the discriminant functions analysis for *Chrysaora fulgida*, *C. hysoscella*, *C. africana* and *C. agulhensis* **sp. nov.**: $\delta_1^2 = 0.96$, $\delta_2^2 = 0.94$. Vector overlays show the relationship between those variables (meristic and standardized morphometric measures) that have a Spearman Rank correlation of > 0.55 with the CAP axes. (VLW = Velar lappet width; RLW = Rhopalial lappet width; MD = Manubrium depth; ML = Manubrium length; Mouth D = Mouth diameter; OW = Ostia width; No. VL = Number of velar lappets; Max OAW = Maximum width of oral arm).

Cnidome

Medusae

Five distinct nematocyst types were observed in the southern coast specimens of *Chrysaora* and *C. africana* while four distinct types occurred within *C. fulgida* (Table 5). The univariate analyses revealed significant differences in a number of measures between nematocysts occurring across these three taxa. For the heterotrichous microbasic euryteles, shaft lengths differed significantly between *C. africana* and the southern coast material (DF = 28, F = 62.91, $p < 0.001$), while no significant differences were found in the capsule lengths or widths. For the atrichous isorhizae, the capsule width (DF = 19, F = 19.19, $p < 0.001$; Tables 6−7) and shaft length (DF = 19, F = 61, $p < 0.001$; Tables 6−7) differed between *C. africana* and the regional material while no differences were observed in the capsule length. For the holotrichous A-isorhizas, capsule length (DF = 60, F = 5.41, $p < 0.001$) and width (DF = 60, F = 5.78, $p < 0.001$) differed across all taxa, while shaft lengths (DF = 60, F = 0.36, $p = 0.69$) did not differ significantly (Tables 6−7). The holotrichous O-isorhizas differed in the capsule length (DF = 60, F = 7.24, $p < 0.001$) and width (DF = 60, F = 4.56, $p = 0.014$) between the three taxa while the shaft lengths did not differ significantly (DF = 60, F = 1.439, $p = 0.245$; Tables 6−7). No significant differences were observed across the remaining nematocysts.

TABLE 5. Widths, lengths and shaft lengths (raw data), of various nematocysts occurring on the tentacles and oral arms of *Chrysaora agulhensis* **sp. nov.**, *C. fulgida* and *C. africana*. All measurements shown as mean ± standard error.

		Measures (µm)		
Species	**Tissue**	**Shaft/tubule Length**	**Length**	**Width**
C. africana	**Oral arm (OA)**			
	Atrichous isorhiza	149.6 ± 1.63	10.1 ± 0.23	7.4 ± 0.16
	Heterotrichous microbasic bi-rhopaloid	51.05 ± 90.4	11.45 ± 0.40	8.1 ± 0.52
	Holotrichous A-isorhiza	80.1 ± 0.9	11.2 ± 0.39	8.4 ± 0.16
	Holotrichous O-isorhiza	116.1 ± 1.61	9.3 ± 0.30	8.9 ± 0.35
	Tentacle (T)			
	Heterotrichous microbasic bi-rhopaloid	159.2 ± 27.36	13.55 ± 0.76	8.4 ±0.52
	Holotrichous O-isorhiza	116.9 ± 6.82	11.2 ± 0.36	10.7 ± 0.30
C. fulgida	**Ephyrae**			
	Heterotrichous microbasic bi-rhopaloid	54.6 ± 1.46	9.9 ± 0.18	8.4 ± 0.27
	Holotrichous O-isorhiza		10.2 ± 0.25	8.8 ± 0.25
	Oral arm (OA)			
	Heterotrichous microbasic eurytele	12.11 ± 0.63	11.89 ± 0.35	8.78 ± 0.49
	Heterotrichous microbasic bi-rhopaloid	56.55 ± 6.74	10.95 ± 0.22	7.75 ± 0.22
	Holotrichous A-isorhiza	13.36 ± 0.43	12.91 ± 0.31	9.45 ± 0.28
	Holotrichous O-isorhiza	68.2 ± 10.48	12.1 ± 0.53	11.6 ± 0.50
	Tentacle (T)			
	Heterotrichous microbasic bi-rhopaloid	112.71 ± 17.5	14.57 ± 0.72	10.38 ± 0.55
	Holotrichous A-isorhiza	79.4 ± 1.50	11.4 ± 0.40	7.4 ± 0.27
	Holotrichous O-isorhiza	128 ± 2.47	11.6 ± 0.54	11 ± 0.85
C. agulhensis	**Ephyrae**			
sp. nov.	Heterotrichous microbasic bi-rhopaloid	-	11.2 ± 0.13	10.3 ± 0.21
	Holotrichous O-isorhiza	-	7.8 ± 0.2	7.4 ± 0.16
	Oral arm (OA)			
	Heterotrichous microbasic eurytele	24.1 ± 0.94	12.81 ± 0.37	9.38 ± 0.56
	Heterotrichous microbasic bi-rhopaloid	67.7 ± 7.32	11.55 ± 0.32	7.7 ± 0.30
	Holotrichous A-isorhiza	53.2 ± 3.93	11.6 ± 0.48	7.8 ± 0.29
	Holotrichous O-isorhiza	95.75 ± 11.85	11.58 ± 1.10	10.42 ± 0.87
	Tentacle (T)			
	Atrichous isorhiza	125.5 ± 1.28	10.3 ± 0.26	6.4 ± 0.16
	Heterotrichous microbasic bi-rhopaloid	135.95 ± 24.24	15.1 ± 0.94	9.7 ± 0.73
	Holotrichous A-isorhiza	82.36 ± 2.54	12.64 ± 0.28	7.91 ± 0.25
	Holotrichous O-isorhiza	114.1 ± 3.54	18.1 ± 1.30	14.7 ± 0.93

For each nematocyst type that occurred in both the oral arms and tentacles, little variability was observed between the length and width of the capsule (Table 6). Significant differences were however observed in the lengths of the shaft/tubules between the two tissue types (Tables 6–7). The oral arms had a comparatively higher diversity of nematocysts (rhopaloids, isorhizas and euryteles) than the tentacles (contained only rhopaloids and isorhizas) (Appendix 3). The Chi-square analyses furthermore revealed significant differences in the relative abundance of nematocysts between taxa (DF = 2, Chi-square = 31.11, $p < 0.001$), and tissue type (DF = 1, Chi-square = 7.20, $p = 0.027$).

TABLE 6. Results of the two-way ANOVA performed between the species *Chrysaora* agulhensis **sp. nov.**, *C. fulgida* and *C. africana* to test for overall differences in the log width, log length and log shaft/tubule length for those nematocysts they had in common. The ANOVA also tested for differences between those nematocysts occurring on both the oral arm and tentacles. (Results considered significant at $p < 0.0051$ after Bonferoni correction, indicated by an asterix).

		Log Length			Log Width			Log Shaft/ tubule Length		
Nematocysts	**Comparisons**	**DF**	***F***	***p***	**DF**	***F***	***p***	**DF**	***F***	***p***
Atrichous isorhiza	*C. agulhensis* **sp. nov.** & *C. africana*	19	0.3	0.59	19	19.19	**< 0.001**	19	136.61	**< 0.001**
	Between tissue	1	0.3	0.59	1	19.19	**< 0.001**		136.61	**< 0.001**
Heterotrichous microbasic eurytele	*C. agulhensis* **sp. nov.** & *C. africana*	29	2.22	0.15	29	0.21	0.65	29	62.91	**< 0.001**
	Between tissue	-	-	-	-	-	-	-	-	-
Heterotrichous microbasic bi-rhopaloid	All species	140	0.67	0.51	140	1.83	0.17	140	1.38	0.26
	Between tissue	140	36.90	**< 0.001**	140	13.62	**< 0.001**	140	29.02	**< 0.001**
Holotrichous O-isorhiza	All species	60	7.24	**< 0.001**	60	4.56	0.01	60	1.44	0.25
	Between tissue	60	9.04	**< 0.001**	60	8.86	**< 0.001**	60	7.61	**< 0.001**
Holotrichous A-isorhiza	All species	60	5.41	**< 0.001**	60	5.78	**< 0.001**	60	0.37	0.69
	Between tissue	60	6.47	**0.01**	60	0.07	**0.79**	60	29.99	**< 0.001**

TABLE 7. Results of the multiple comparisons post hoc ANOVA, performed between those nematocysts and species that were significantly different (see Table 6). Only nematocysts which showed differences in the two-way ANOVA analysis, and were present in more than two species have been included here (results considered significant at $p < 0.0046$ after Bonferoni correction).

			heterotrichous microbasoc bi-rhopaloid			**holotrichous-O-isorhiza**			**holo-A-isorhiza**		
Variable	**Species**		Mean	SE	Sig.	Mean	SE	Sig.	Mean	SE	Sig.
Width log	*C. africana*	*C. fulgida*	-0.08	0.02	0.00	-0.06	0.03	0.06	0.00	0.02	1.00
		C. agulhensis **sp. nov.**	-0.06	0.02	0.02	-0.09	0.02	0.00	0.03	0.02	0.24
	C. fulgida	C. africana	0.08	0.02	0.00	0.06	0.03	0.06	0.00	0.02	1.00
		C. agulhensis **sp. nov.**	0.03	0.02	0.60	-0.03	0.02	0.90	0.03	0.01	0.10
	C. agulhensis **sp. nov.**	*C. africana*	0.06	0.02	0.02	0.09	0.02	0.00	-0.03	0.02	0.24
		C. fulgida	-0.03	0.02	0.60	0.03	0.02	0.90	-0.03	0.01	0.10
Length log	*C. africana*	C. fulgida	-0.09	0.02	0.00	-0.06	0.03	0.10	-0.04	0.02	0.12
		C. agulhensis **sp. nov.**	-0.02	0.02	1.00	-0.13	0.03	0.00	-0.03	0.02	0.14
	C. fulgida	*C. africana*	0.09	0.02	0.00	0.06	0.03	0.10	0.04	0.02	0.12
		C. agulhensis **sp. nov.**	0.08	0.02	0.00	-0.07	0.03	0.06	0.00	0.01	1.00
	C. agulhensis **sp. nov.**	*C. africana*	0.02	0.02	1.00	0.13	0.03	0.00	0.03	0.02	0.14
		C. fulgida	-0.08	0.02	0.00	0.07	0.03	0.06	0.00	0.01	1.00
Tubule log	*C. africana*	*C. fulgida*	-0.13	0.09	0.52	0.16	0.06	0.04	0.41	0.02	0.00
		C. agulhensis **sp. nov.**	0.16	0.09	0.26	0.06	0.06	0.93	0.09	0.02	0.00
	C. fulgida	*C. africana*	0.13	0.09	0.52	-0.16	0.06	0.04	-0.41	0.02	0.00
		C. agulhensis **sp. nov.**	0.29	0.09	0.01	-0.09	0.06	0.37	-0.33	0.02	0.00
	C. agulhensis **sp. nov.**	*C. africana*	-0.16	0.09	0.26	-0.06	0.06	0.93	-0.09	0.02	0.00
		C. fulgida	-0.29	0.09	0.01	0.09	0.06	0.37	0.33	0.02	0.00

Ephyrae

Two distinct types of nematocysts were found within the ephyrae of *Chrysaora fulgida* and southern coast *Chrysaora*: heterotrichous microbasic bi-rhopalods and holotrichous O-isorhiza. For both these nematocyst types, the results of the two-way ANOVA revealed the capsule length and width to differ significantly between taxonomic units, while the lengths of the shafts did not differ significantly (Table 6). The ANOVA also indicated shaft and capsule lengths to differ significantly between the ephyrae and medusae for both nematocyst types, however capsule widths often indicated no significant differences (Table 6). The cnidome of ephyrae of *C. africana* was not examined.

DNA analysis

Gene characteristics

For cytochrome *c* oxidase subunit I (COI) a 620 bp region was amplified from seven specimens of the *Chrysaora* collected from the south coast, three *C. africana* and seven *C. fulgida* (five collected off the coast of Namibia and two collected off the coast of South Africa) specimens (Appendix 1): this was subsequently truncated to 616 bp. The parsimony analysis revealed 194 (31.5%) characters to be parsimony informative, 22 (3.5%) characters were variable but uninformative and 400 (65%) were invariable for the COI gene region. For the 18S gene region, a 1800 bp region was amplified from six *C. fulgida*, three *C. africana* and five of the *Chrysaora* collected along the southern coast of South Africa: this was subsequently truncated to 1745 bp. The parsimony analysis revealed 1612 (92%) sites to be invariable, while 87 (5%) were considered parsimony informative and 46 (3%) were variable but uninformative. For the ITS region which included ITS1, ITS2 and 5.8S, a 752 bp amplicon was amplified from six *C. fulgida*, three *C. africana* and five of the *Chrysaora* collected along the southern coast of South Africa: this was subsequently truncated to 655 bp and separated into individual gene regions (i.e. ITS1, ITS2 and 5.8S) as described previously. For ITS1 a total of 288 bp were obtained and the parsimony analysis revealed 65 (23%) characters to be parsimony informative while 187 (65%) were constant and 36 (13%) were variable but uninformative. For ITS2, a total of 210 bp were obtained and the parsimony analysis revealed 77 (37%) to be parsimony informative with 12 (6%) variable but uninformative and 121 (58%) invariable, while the 5.8S region contained a total of 157 bp and 5 (3.2%) characters were considered informative and 150 (95.5%) invariable. A number of genetic sequences were also obtained from GenBank and included in these analyses (indicated by the GenBank ID at the end of sequence names).

TABLE 8. Pairwise genetic distances for the mtDNA (COI) and nucDNA (18S, ITS1, ITS2 and 5.8S) for the monophyletic clades of *Chrysaora*. Distances are represented as mean ± standard error. The average number of nucleotide substitutions per site, between taxa (Dxy) is also shown. Individual *p*_distance matrices for each region can be found in supplementary tables S1, S2, S4 and S5.

Species		nucDNA		mtDNA	
		Dxy	***p_distance***	**Dxy**	***p_distance***
C. africana	*C. fulgida*	0.064	0.035 ± 0.005	0.168	0.165 ± 0.015
C. africana	*C. agulhensis* **sp. nov.**	0.059	0.029 ± 0.004	0.171	0.171 ± 0.015
C. africana	*C. hysoscella*	0.062	0.033 ± 0.004	0.179	0.179 ± 0.015
C. agulhensis **sp. nov.**	*C. fulgida*	0.015	0.016 ± 0.003	0.039	0.029 ± 0.006
C. agulhensis **sp. nov.**	*C. hysoscella*	0.023	0.019 ± 0.003	0.072	0.067 ± 0.010
C. fulgida	*C. hysoscella*	0.016	0.010 ± 0.002	0.076	0.074 ± 0.011

Pairwise divergence and phylogenetic reconstruction

The Bayesian analysis of the COI data revealed the presence of four monophyletic lineages (Fig. 2), which supports the complete distinction of *Chrysaora africana* and *Chrysaora fulgida* (minimum pairwise differences = 14.7%). It also showed the southern coast specimens of *Chrysaora* to be genetically distinct from *C. africana* and although it did form a clade with *C. fulgida*, there appears to be a clear separation between the sequences of both (bootstrap = 100; posterior probability = 1). The mtDNA sequence data (Table 8 & S1) showed a minimum of 14.2% pairwise sequence differences between the south coast material and *C. africana*, a minimum of 2.2% pairwise sequence dif-

ferences between the south coast material and *C. fulgida*, and a minimum of 5.8% pairwise sequence differences between the south coast material and *C. hysoscella*.

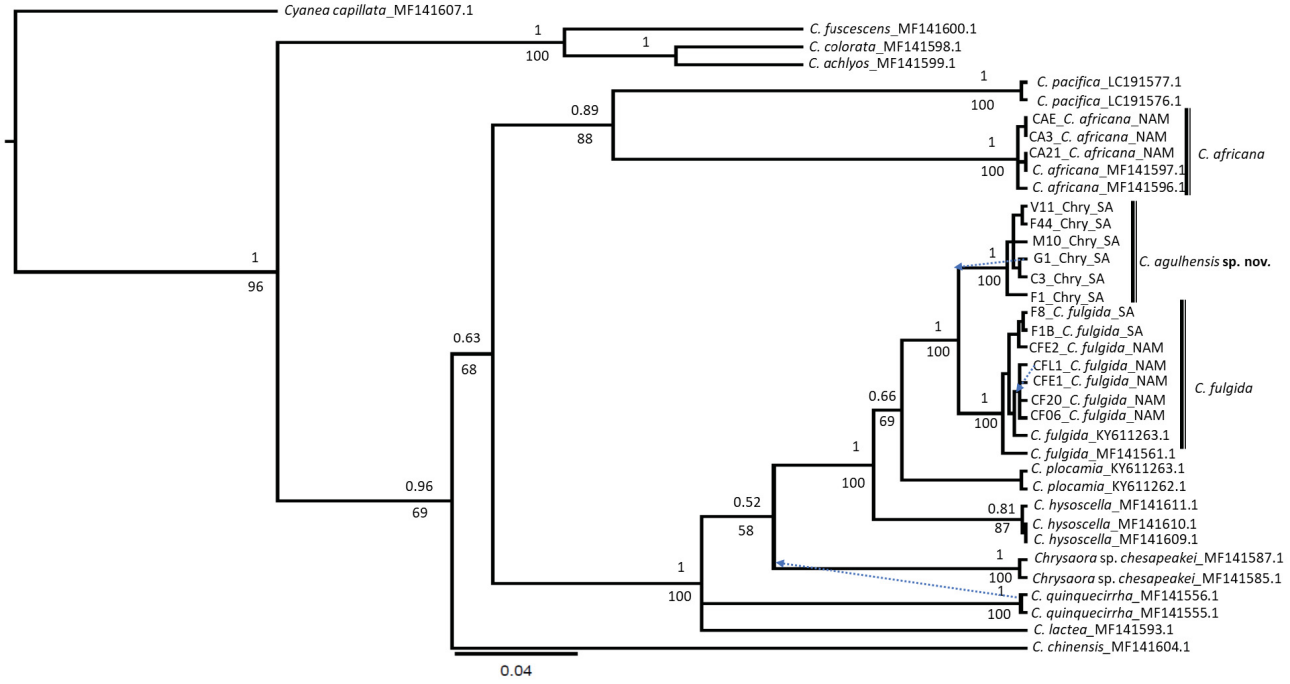

FIGURE 2. Rooted Bayesian COI tree using TPMuf+I+G model of evolution. Geographic information on collecting sites is provided in Table 1 & Appendix 1. Posterior probabilities (BY) and bootstrap support values (ML) are given above and below branches respectively. Dotted lines indicate alternative topologies present in Maximum Likelihood analyses.

The parsimony analysis of the 18S data, similarly to the mtDNA, indicated four monophyletic groups between *Chysaora africana*, *Chrysaora fulgida*, *Chrysaora hysoscella* and the *Chrysaora* collected along the South coast (S2–S3). Interestingly, the nuclear DNA (nucDNA) sequence data (Table 8 & S2), showed less variation between *C. africana* and those collected from the south coast and in this case formed a clade with the former. Here we see *C. africana* and the southern coast specimens separating from *C. fulgida* entirely, with all pairwise differences appearing significant (all >1% S2–S3). This however did not occur in the ITS1, ITS2 or 5.8S gene regions when analysed (S4–S7 (5.8S tree not shown)). Here, as in the mtDNA, they formed a clade with *C. fulgida*. The *Chrysaora* collected along the south coast again showed very little variability between it and *C. fulgida* for these gene regions (all <2%) but still appeared to separate from *C. africana* and *C. fulgida* in all analyses (see Figs 2 & S1–S7).

The result of the concatenated (nucDNA) analysis is shown in Fig. 3 (species tree). It reveals a clear separation between all the putative species of *Chrysaora* found in the E Atlantic with high bootstrap support (100%) and posterior probabilities (1). Results of the time-calibrated time tree shows a recent split between *C. fulgida*, and the SA material, indicating a potential divergence time of only 200 000 (CI: 0.00; 0.49) years ago and a split between these and *C. hysoscella* between 4.17 Mya (CI: 0.39; 9.79) and 390000 (CI: 0.04 ; 0.90) years ago.

TABLE 9. Estimates of haplotype diversity (*h*) and nucleotide diversity (π) for the mtDNA (COI) and nucDNA (18S, ITS1, ITS2 and 5.8S) for *Chrysaora fulgida*, *C. africana*, *C. agulhensis* **sp. nov.** and *C. hysoscella*.

mtDNA				nucDNA				
Species	**No. of haplotypes**	***h***	**π**	**No. segregating sites**	**No. of haplotypes**	***h***	**π**	**No. segregating sites**
C. africana	3	0.8	0.003	3	3	1	0.001	4
C. fulgida	8	0.972	0.007	15	3	0.524	0.002	14
C. agulhensis **sp. nov.**	6	1	0.008	12	5	1	0.003	11
C. hysoscella	2	0.667	0.001	1	2	1	0.009	18

Upon analysing the haplotype diversity for the mtDNA, all species appeared to have a high level of diversity (all >0.7; Table 9) with only *C. hysoscella* showing a lower haplotype diversity (0.67; Table 9). The nucDNA showed a similar trend however *C. fulgida* showed a markedly lower haplotype diversity (0.52).

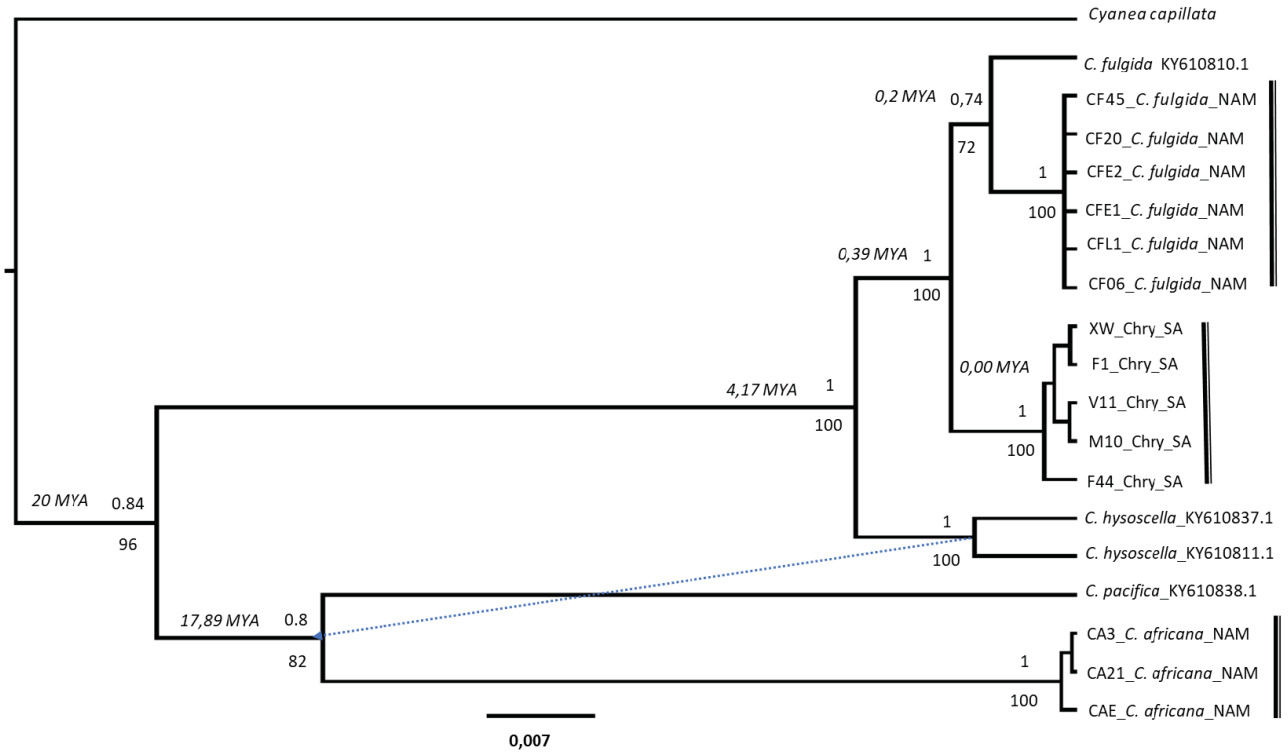

FIGURE 3. Rooted Bayesian species tree for the concatenated nuclear dataset of 18S, ITS1, ITS2 and 5.8S based on the GTR+I+G model of evolution. Posterior probabilities (BY) and bootstrap support values (ML) are given above and below branches respectively. Dotted lines indicate alternative topologies present in Maximum Likelihood analyses. Estimated divergence times, as determined by a time calibrated (RelTime) analysis, are represented on nodes as MYA.

Discussion

The recent recognition and effective resurrection of *Chyrsaora africana* from *C. fulgida* (Bayha *et al.* 2017) is supported and detailed in the following section, but their prior synonymy appears to follow the generally troubled taxonomic history of the genus (Morandini & Marques 2010). This undoubtedly reflects the poor nature of the original descriptions, an over-reliance on morphology in species delineation and a difference in opinion regarding species identity. This confusion is not unique to *Chrysaora* but, appears to be a general problem in the taxonomy of Scyphozoa (e.g. Dawson & Jacobs 2001; Gerswhin & Collins 2002; Dawson 2003; Holland *et al.* 2004) and, can perhaps be linked to their relatively simple and conserved morphology. Molecular methods are a particularly useful tool that can be used to separate species, and their recent employment has led not only to the recognition of a number of cryptic or previously misidentified species (Dawson & Jacobs 2001; Dawson 2003; Holland *et al.* 2004; Dawson 2005; Bayha *et al.* 2017) but has also supported changes to lower-level phylogenies (Bayha *et al.* 2010). In a well cited paper, Dawson (2003) suggested that in order to move our understanding of scyphozoan taxonomy forward, and thereby improve our knowledge of diversity, we need to draw on more lines of evidence than morphology alone. Such evidence should certainly embrace molecular markers (e.g. Gómez-Daglio & Dawson 2017) and the cnidome (Carlgren 1940; Dawson 2003), but could also include information about ecology.

The data presented here, as they pertain to *C. fulgida* and to the south coast specimens of *Chrysaora*, are particularly interesting in this regard. There are clear and significant differences between the two in terms of morphology, meristics and cnidome, and subtle differences in ephyrae (all detailed below). However, the pairwise sequence differences in COI are lower (2.9%) than what is generally considered to be representative of species-level differences (e.g. Abboud *et al.* 2018). Abboud *et al.* (2018) only used molecular methods in their analyses and stressed

that "DNA barcoding has limitations of differentiating between populations which diverged recently" (Abboud *et al.* 2018: pp 210). Gómez-Daglio & Dawson (2017) further reminded us that barcoding gaps within Discomedusae are highly heterogenous, with discontinuities frequently detected and, stressed that barcoding gaps may be particularly variable within the Pelagiidae. The results of the timetree (Fig. 3) estimates the divergence time between *C. fulgida* and the South African morphotype at only 200 000 years ago. This is an extremely recent divergence and does stress that these morphotypes diverged recently and could potentially explain the low levels of genetic differences.

Indigenous species have evolved within, and display adaptations to, the environments in which they are located. Behaviours, ecologies and lifecycles are cued to changes in the environment and few species naturally show distributions across very wide environmental gradients. Whilst fish species such as sardines (*Sardinops sagax*), anchovies (*Engraulis encrasicolus*) and hakes (*Merluccius capensis, M. paradoxus*) may have distributions that encompass the whole of the productive region around the SW coasts of southern Africa, their very mobility allows them to track environmental optima (Hutchings *et al.* 1998; van der Lingen *et al.* 2006). Indeed, this may account, in part, for recent shifts in distribution that mirror, in part, changes in the local thermal environment (Hutchings *et al.* 1998; van der Lingen *et al.* 2006). Immobile species, on the other hand, or species that have an immobile life history stage (such as *Chrysaora*), are not "so lucky" in this regard, and need to evolve and adapt to their prevailing environments. We have detailed differences in the west and south coast environments previously: they are significant (see Lutjeharms & Cooper 1996; Awad *et al.* 2002; Hutchings *et al.* 2009; Vousden *et al.* 2012). The south coast of South Africa is also different from that experienced along the east coast (Awad *et al.* 2002) and it is perhaps no wonder that for many meroplanktonic taxa, the south coast represents a centre of regional endemism (Awad *et al.* 2002). Indeed, greatest levels of South African marine invertebrate endemism are noted in the area between False Bay and Port Elizabeth, for taxa such as the: octocorals, chitons, bivalves, opistibranch gastropods, polychaetes, brachyuraans, echinoderms as well as ascidians (Awad *et al.* 2002; Griffiths *et al.* 2010).

It is our belief, given these arguments, and the arguments presented by Dawson (2003) for using multiple lines of evidence in species delineation, that the south coast specimens of *Chrysaora* should be recognised as a separate species from *C. fulgida*. In making this decision, we also need to formally resurrect *C. africana*, and thoroughly describe all species. Formal descriptions of each follow.

SYSTEMATICS

Sub-Class DISCOMEDUSAE Haeckel, 1880

Order SEMAEOSTOMEAE L. Agassiz, 1862

FAMILY Pelagiidae Gegenbaur, 1856

GENUS *Chrysaora* Péron and Lesueur, 1810

SPECIES *Chrysaora agulhensis* sp. nov.

[FIGS 3a–e; 4a–d; 5; 6]

Type material. Holotype: South Africa: False Bay: MB-A088455 (14.8 cm in diameter, 22 June 2014, preserved in 5% formaldehyde in ambient seawater, Fish Hoek beach, South Africa, opposite train station (34.14°S 18.43°E), V. Ras col.). **Paratypes**: **South Africa: False Bay: MB-A088456** (~12 cm in diameter, 22 April 2014, preserved in 5% formaldehyde in ambient seawater, Fish Hoek beach, South Africa, opposite train station (34.14°S, 18.43°E), V. Ras col.); **False Bay: MB-A088457** (~13 cm in diameter, 13 November 2012, preserved in 5% formaldehyde in ambient seawater, Whale Rock off Robben Island, South Africa, D. Cox col. (33.81°S, 18.37°E).

Examined material: Holotype: (MB-A088455). Paratypes: (MB-A088456); (MB-A088457).Seven specimens collected by boat at Whale Rock off Robben Island in November 2012 (33.81°S, 18.37°E); 11 beach stranded specimens collected at Muizenberg in April 2014 (34.11°S, 18.47°E) (MB-A088458); Four specimens collected by net at Gouritzmond in October 2014 (34.35°S, 21.89°E); Ten stranded specimens collected at Zewenwacht Beach in March 2011 (34.11°S, 18.79°E); Five ephyrae (MB-A088460) and five polyps (MB-A088459) obtained following

the settlement of planulae from specimens of medusa collected at Whale rock off Robben Island; Three medusae from False Bay, collected in 2012 (34.13°S, 18.44°E: 34.10°S, 18.48°E).

Type locality. Fish Hoek beach, False Bay, Cape Town, South Africa.

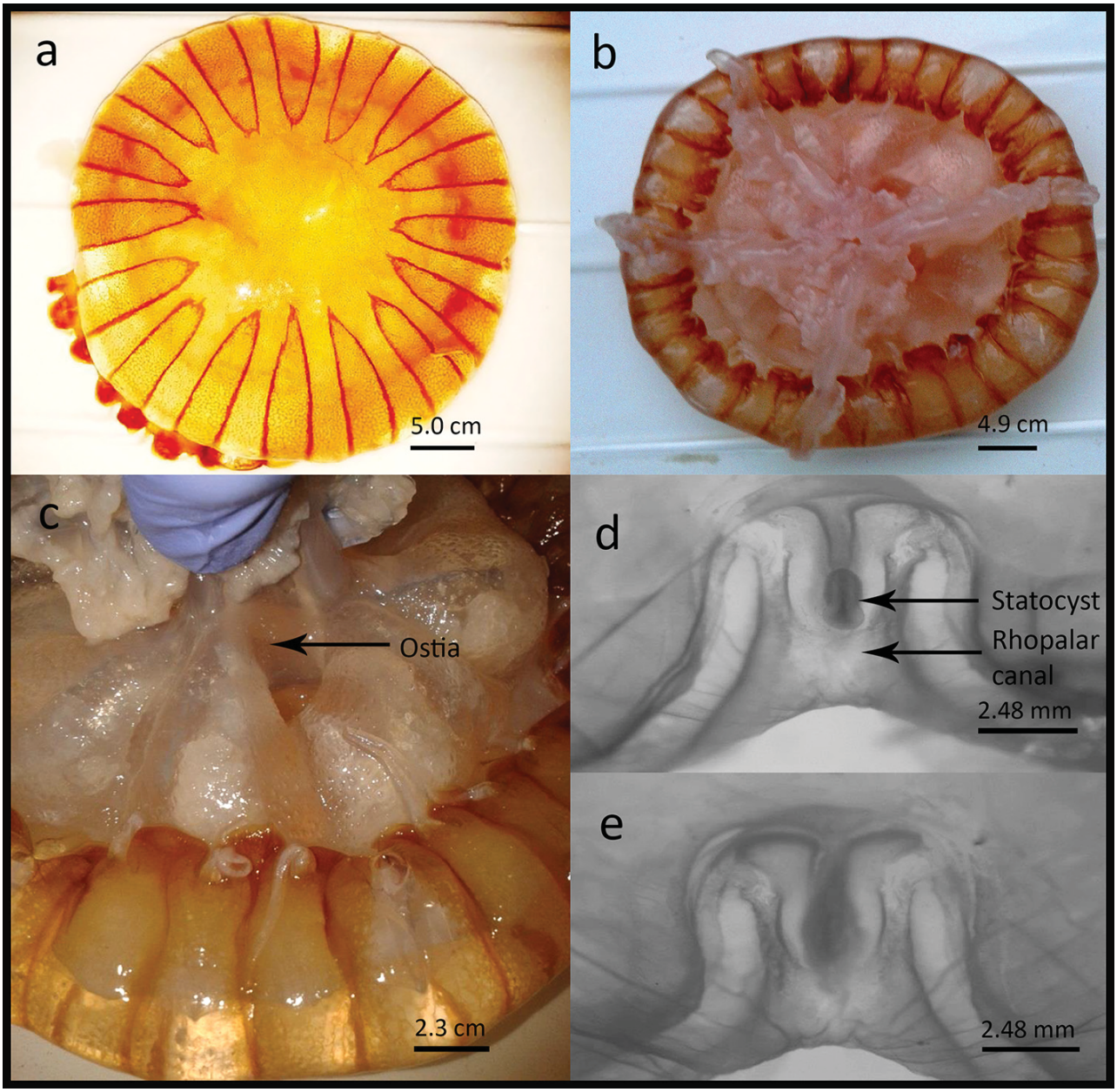

FIGURE 4. Photographs of the Holotype specimen (MB-A088455) of *Chrysaora agulhensis* **sp. nov.** submitted to the South African Natural History Museum, collected at False Bay (Fish Hoek), South Africa in June 2014, showing a) the exumbrellar surface with characteristic star-shaped colouration and b) the subumbrellar surface showing colour and length of the oral arms, colour of manubrium as well as the shape of the velar and rhopalial lappets. The shape of the tentacular and rhopalial pouches, showing radial septum fusing at periphery of rhopalial lappets can also be seen in this image. In c) the arrangement of the primary and secondary tentacles (2:1:2) are shown, with the shape and size of the ostia also clearly visible. Enlarged images of the rhopalium which illustrates: d) the ventral view showing the hood and e) the dorsal view showing the statocyst and rhopalal canal.

Distribution. Range stretches from Table Bay along the west coast of South Africa towards Port Elizabeth along the south east coast of South Africa (Agulhas Bank): endemic.

Diagnosis. *Chrysaora* of medium size; 32 rounded marginal lappets, four per octant; no more than 24 persistent tentacles; tentacles laterally flattened with pronounced bases, and ribbon-like; oral arms longer than bell, folded spirally at base; characteristic star shape pattern on exumbrella surface always visible, created by the radial pat-

tern of deep maroon/purple triangles; white spots scattered across the surface of the exumbrella; mouth becomes substantially larger as organism grows. Lappets with network of gastrovascular canals. Oral arms spirally arranged basally.

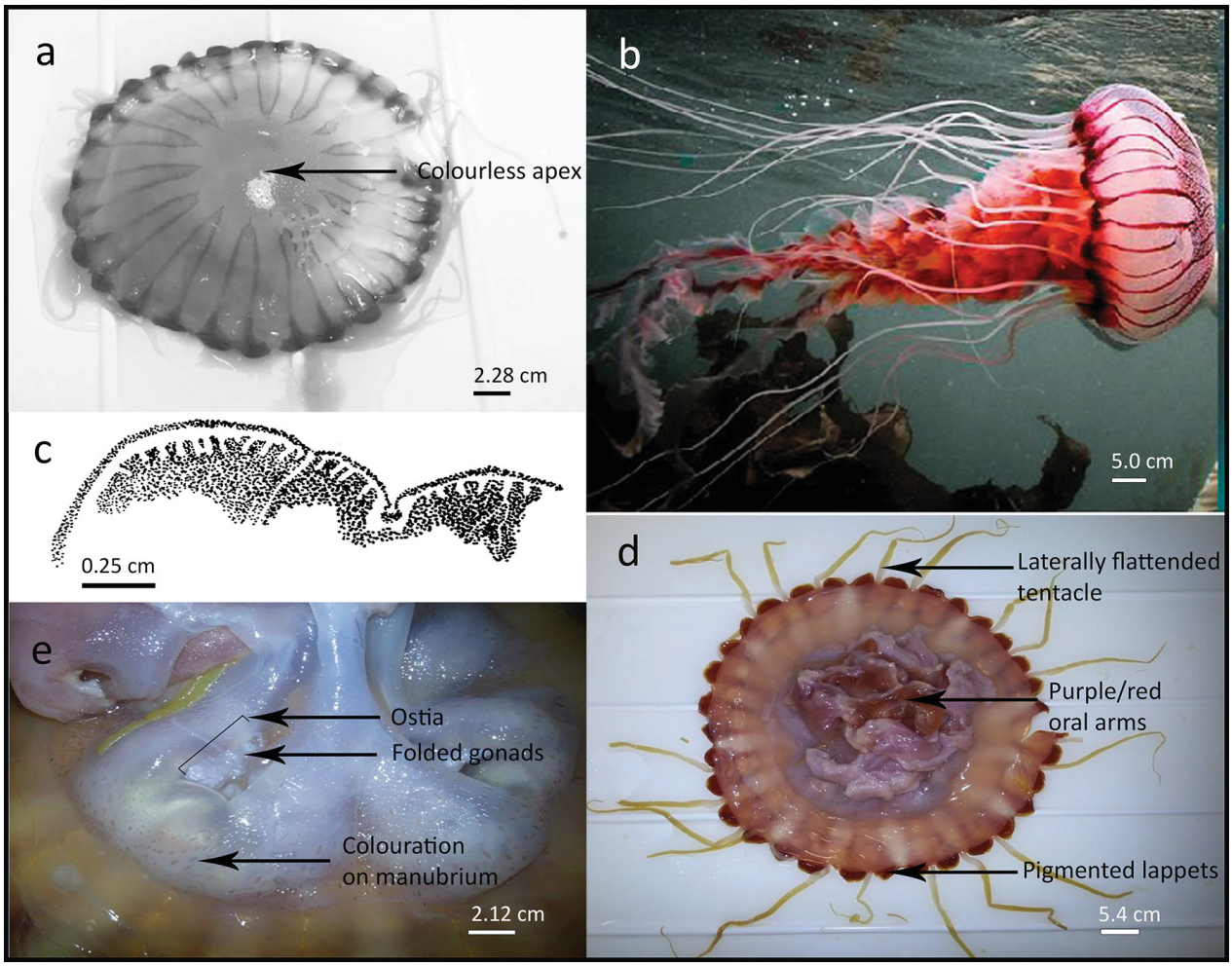

FIGURE 5. Photographs of *Chrysaora agulhensis* **sp. nov.** collected at Whale Rock during November 2012 showing a) exumbrellar view of medium sized preserved specimen (12 cm) (Paratype: MB-A088456) displaying the lack of pigmentation on the central disk and shape of gonads, b) side-view of a larger specimen in situ displaying deep purple colouration of the central apex, long trailing oral arms and ribbon-like tentacles, c) enlarged image of the finger-like network of canals found toward the periphery of the rhopalial lappets and, d) subumbrella image of a large (> 20 cm) preserved specimen, showing maroon/purple colouration of the manubrium and e) uniform pigmentation found on the manubrium of larger specimens. Photograph in b) with kind permission from Peter Southwood, recreational underwater photographer.

Holotype description. Umbrella hemispherical in shape, diameter 14.8 cm. Exumbrella with small raised nematocyst warts, slightly granular, translucent brown in colour (preserved) (Fig. 4a), with 16 elongated triangles extending outward from central apex on bell; apices of triangles pointed toward central apex (Fig. 4a); colouration of triangles alternate between darker brown pigmentation and little to no pigmentation, forming characteristic star-shaped pattern; central apex visible as an unpigmented, translucent circle (Fig. 4a); white spots scattered throughout exumbrellar due to raised nematocyst warts. Umbrella centrally thickened; central mesoglea 3.5 x thicker than margin. Umbrella margin cleft into 32 rounded lappets, four lappets per octant: two rhopalial lappets situated next to rhopalium and two velar lappets situated between rhopalial lappets (Fig. 4c). Rhopalial lappets not as wide as velar lappets, thus velar lappets appearing elongated while rhopalial lappets appear pointed; lappets equally pigmented on upper and lower surface, appearing dark brown.

Rhopalia: eight rhophalia situated in deep clefts between adjacent rhopalial lappets, project from margin of umbrella into rhopalar canal. Rhopalium protected by sensory niche and an extension from subumbrellar margin forms a protective layer or “hood” above rhopalium (Fig. 4d). Base of rhopalium attached to a ridge, running

to proximal wall of sensory niche. Thickened endoderm covers surface of sensory niche on subumbrella, thickest along proximal wall (Fig. 4e). Thickened endoderm extends outwards for short distance (equal in length to rhopalar canal) (Appendix 3) alongside lappets. Deep, cone shaped sensory pit situated above rhopalium. Rhopalium itself consists of a statocyst, (Figs 4d–e) and short, hollow, basal stem (approximately equal in length to statocyst) (Appendix 3). Basal stem clasped by subumbrellar bulb and receives rhopalial canal which is approximately twice as long as the statocyst (Figs 4d–e, Appendix 3). No ocelli observed.

One primary tentacle found in each octant, located in clefts between adjacent velar lappets, with two well-developed secondary tentacles situated in clefts between adjacent velar and rhopalial lappets (arrangement 2:1:2), for a total of 24 tentacles (Fig. 4c). Tentacles laterally flattened (not circular), solid in cross-section and "ribbon-like"; tentacles less pigmented on ventral surface and cream in colour, light brown on dorsal surface; tentacles cream and unpigmented at base, becoming more pigmented distally and light brown toward tentacle tip. Subumbrella translucent white and smooth; gastrovascular pouches covering central stomach granular (Fig. 4c); radial septa arise from periphery of central stomach, dividing gastrovascular cavity into 16 pouches; septa span entire length of circular muscle and fuse at periphery of rhopalial lappets; tentacular pouches dilate and contract distally; rhopalial pouches contract and dilate distally. Manubrium and gastrovascular pouches cream in colour; manubrium arising from central stomach forms thin, tubular, slightly elongated structure with thickened mesoglea; oral opening (mouth) cruciform and situated in centre of manubrium; manubrium wall divided into four oral arms distally. Oral arms cream and translucent (Fig. 4b), lancelet-shaped, with distal portion of oral arm much thinner than proximal and central portion; V-shaped in cross section; oral arms spiralled proximally, becoming less spiralled distally; oral arms 15% longer than bell diameter. Basal portion of manubrium fused and thickened to form four gonadal pouches with four oval orifices or ostia situated between them (Fig. 4c); gonads attached to periphery of ostia and highly folded/convoluted into semi-circular shape; one ostia situated between two adjacent gonads. No sperm sacs, quadralinga or gastric cirri observed.

Description of other specimens and additional data

Medusae: All material examined was preserved; no live specimens were examined except from photographs. The umbrella diameter (UD) of investigated material ranged from 2.95 cm to 20.75 cm, all hemispherical in shape (slightly flattened in smaller specimens) and all showing pronounced pigmentation. Central apex always unpigmented and translucent in smaller specimens (Fig. 5a), but becoming more pigmented, though still pattern-free, in larger specimens (Fig. 5b). White spots scattered throughout the exumbrella, but become more clearly visible in larger specimens (Fig. 5b). The mesoglea becomes proportionately thicker as the specimen grows. Marginal lappets strongly pigmented, with a series of canals around the outer edges that are not well defined (Fig. 5c). Subumbrella becomes slightly maroon/purple in larger specimens (Fig. 5d). Twenty-four persistent tentacles present; all strap-like with relatively broad base; white in colour but may display pigmentation laterally Manubrium and gastrovascular pouches cream in colour, however the largest specimens display uniform pigmentation on the pouches, with pigmentation appearing as slight brown oval spots (Fig. 5e). The oral arms are spirally folded at the base, becoming linear distally; pale in colour, though edges and frills are maroon/purple, with some specimens displaying some maroon/purple colouration in the central portions as well (Fig. 5b). Oral arms are also darker at the base in the larger specimens and lose colour distally (Fig. 5b). Oral arms typically 15% to 25% longer than UD and become proportionately longer as the jellyfish grows. No sperm sacs, quadralinga or gastric cirri were observed in any of these specimens. Sexes are separate. All colouration observed became a dark brown in specimens preserved for more than two years.

Correlation analyses between maximum UD and meristic as well as morphometric features were either constant (most meristic features) or significantly correlated with specimen diameter. Six standardised measures showed size dependency, including the lengths of velar and rhopalial lappets, diameter of the mouth, manubrium length and inter-ostial width: all others were size-invariant.

Polyp: Polyps of *C. agulhensis* **sp. nov.** were reared from material collected from Whale Rock (33.81°S, 18.37°E). Typically, conical in shape, up to 3.5 mm in height (Fig. 6). Oral disk roughly half the length of the polyp (Appendix 3). Possesses up to 16 tentacles, up to five times the length of the polyp (Appendix 3); with four gastric septa and a cruciform mouth. White in colour unless strobilating in which case the upper half becomes brown (Fig. 6).

FIGURE 6. Enlarged images of the polyps of *Chrysaora agulhensis* **sp. nov.**, settled from adult medusae collected at Robbin Island, South Africa in 2013: image illustrating two fully grown polyps; one strobilating (left) and one not strobilating (right).

FIGURE 7. Enlarged images of the cultured ephyrae of *C. agulhensis* **sp. nov.**, taken unfed, at a) two days post liberation, b) two weeks post liberation (indicating size of mouth) and c) two weeks post liberation (whole ephyrae). Lappets stems, lappets, nematocyst clusters and gastric filaments clearly visible.

Ephyrae: At one to 14-days post liberation (stage 0): total body diameter of 2.35 mm ± 568.3 µm, central disk diameter of 750 ± 322.3 µm and manubrium 480 ± 487.9 µm in length. Ephyra possessing eight elongated lappet stems containing rhopalial canals, each bearing two rhopalial lappets thus containing 16 round, spatula like lappets (Figs 7a–c). Lappet length approximately equal to length of stem (Appendix 3). Rhopalial canals forked. Rhopalia situated in clefts between pairs of rhopalial lappets at end of each lappet stem (Fig. 7a). Statocysts dark and clearly visible, with little to no protection (Figs 7a–c). Four gastric filament sockets present with one to two gastric filaments

and no tentacle buds or tentacles observed. Manubrium prominent, relatively wide and fairly long, approximately 55% of the central disk diameter (Figs 7a–c, Appendix 3). Nematocyst clusters situated at the base of the lappets and along rhopalial and velar canals. Ephyrae generally unpigmented, transparent with some light brown pigmentation due to nematocysts and some thickened areas along canals. Nematocysts: Approximately 70% of all nematocysts found within the ephyrae were holotrichous O-isorhizas (L = 7.8 ± 0.2 μm; W = 7.4 ± 0.16 μm), while the remaining 30% constituted heterotrichous microbasic bi-rhopaloids (L = 11.2 ± 0.13 μm; W = 10.3 ± 0.21 μm).

Cnidome: See Table 5. Relative abundances: approximately 68–74% of all nematocysts were heterotrichous microbasic bi-rhopaloids, roughly 24% were holotrichous O-isorhizas while the remainder was made up of a small combination of holotrichous A-isorhiza and hetrotrichous microbasic euryteles, with oral arms containing a lower overall abundance of nematocysts than the tentacles in all specimens.

Haplonemes

Holotrichous A- and O- isorhiza–Oval/circular shaped capsule with no prominent shaft visible within the undischarged capsule (Figs 8a–b). Tubule inverted and isodiametric, beginning to form a coil close to the aperture. The coils then form loops from wall to wall perpendicularly within the capsule (Figs 8a–b). Tubule is tightly coiled and usually more than 10 times the length of the capsule (Table 5). The tubule supports spines of uniform length throughout (Figs 7c–d). Here, "A" indicates a more oval, leaf-like shape (Fig. 8a), while "O" indicates a more circular/rounded shape (Fig. 8b).

Atrichous isorhiza–Oval shaped capsule with no visible, prominent shaft within the undischarged capsule. The tubule is inverted and isodiametric and begins to form a coil close to the aperture. The coils then form loops from wall to wall perpendicularly within the capsule. Tubule is tightly coiled and is usually more than eight times the length of the capsule: without spines (Fig. 8e).

Heteronemes

These nematocysts are distinguished from haplonemes by the presence of a prominent, clearly visible shaft within the unfired capsule (Figs 9a & 9c).

Heterotrichous microbasic bi-rhopaloid–In the undischarged capsule, the shaft generally forms a straight line or axial rod in the centre of the capsule and is microbasic with a relatively long tubule (Table 5, Fig. 9a). Two distinct dilations are also visible on the shaft, one at the base close to the aperture and one at the distal end. These shafts typically have large, loosely set spines, while the tubule bears smaller, more closely set spines (Fig. 9b). Tubules are often tightly coiled in the undischarged capsule.

Heterotrichous microbasic euryteles–Euryteles have broad and prominent shafts both within the undischarged capsule and upon discharge (Figs 9c–d). Within the capsule the shaft forms a straight line or axial rod across the centre of the capsule (length-wise) and is less than three times the length of the capsule (Figs 9c–d). The short distal tubule makes the first loop toward the aperture of the capsule directly after the end of the shaft. Heterotrichous euryteles (Fig. 9d) supports large spines throughout the shaft and smaller spines are present on the tubule.

Biological data: None available.

Etymology. "agulhensis" referring to its distribution across the Agulhas Bank along the South coast of South Africa.

SPECIES *Chrysaora africana* **(Vanhöffen, 1902)**

[FIGS: 10a–e]

Synonymy

Dactylometra africana Vanhöffen 1902: 40 (original description), Pl. IV fig. 20 (medusa). Mayer 1910: 588 (description), fig. 373 (medusa, figure reproduced from Vanhöffen, 1902). Bigelow 1913: 91 (mention, similarities with *C. quinquecirrha*–never more than 5 tentacles per octant). Stiasny 1939: 174–182 (description; *D. africana* probably an older *fulgida*), fig. 2 (medusa, reproduction of original figure), figs 3–7 (medusa, aboral view of octants) [South Africa]. Ranson 1949: 142–143 (description) [Angola, Mauritania, Guinea-Bissau, Namibia]. Kramp 1955: 297 (synonymy), 298 (*D. africana* = *D. quinquecirrha*; considered the synonymy *C. fulgida* = *D. africana* as doubtful), 309–310 (mention, *D. africana* = *C. quinquecirrha*). Thiel 1966: 19–22 (description), Pl. III fig. 5 (rhopalium) [Point Noire–Congo].

Chrysaora africana: Kramp 1961: 323–324 (synonymy). O'Sullivan 1982: 29 (mention). Gershwin & Collins 2002: 128 (mentioned as nominal species with insufficient data). Bayha *et al.* 2017 (resurrected as separate species).

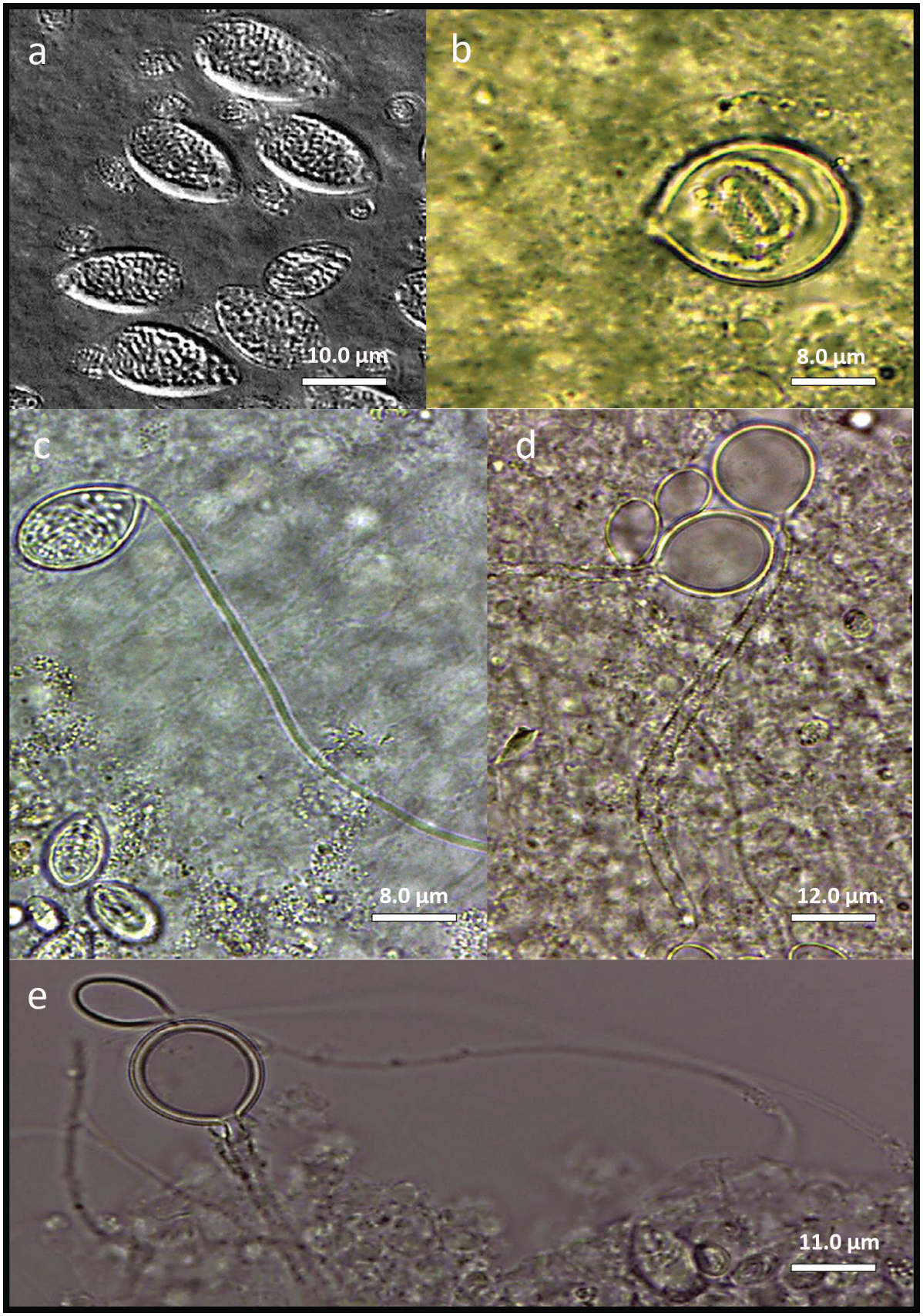

FIGURE 8. Microscopic images (1000 ×) of the isorhiza nematocysts occurring on the oral arms/tentacles of *Chrysaora agulhensis* **sp. nov.**, *C. fulgida* and *C. africana*: a–b) undischarged A and O-isorhiza from the oral arm of *C. fulgida*; c) discharged holotrichous A-isorhiza from the oral arm of *C. agulhensis* **sp. nov**.; d) discharged holotrichous O-isorhiza from the oral arm of *C. agulhensis* **sp. nov.** and e) discharged atrichous anisorhiza from the oral arm of *C. africana*.

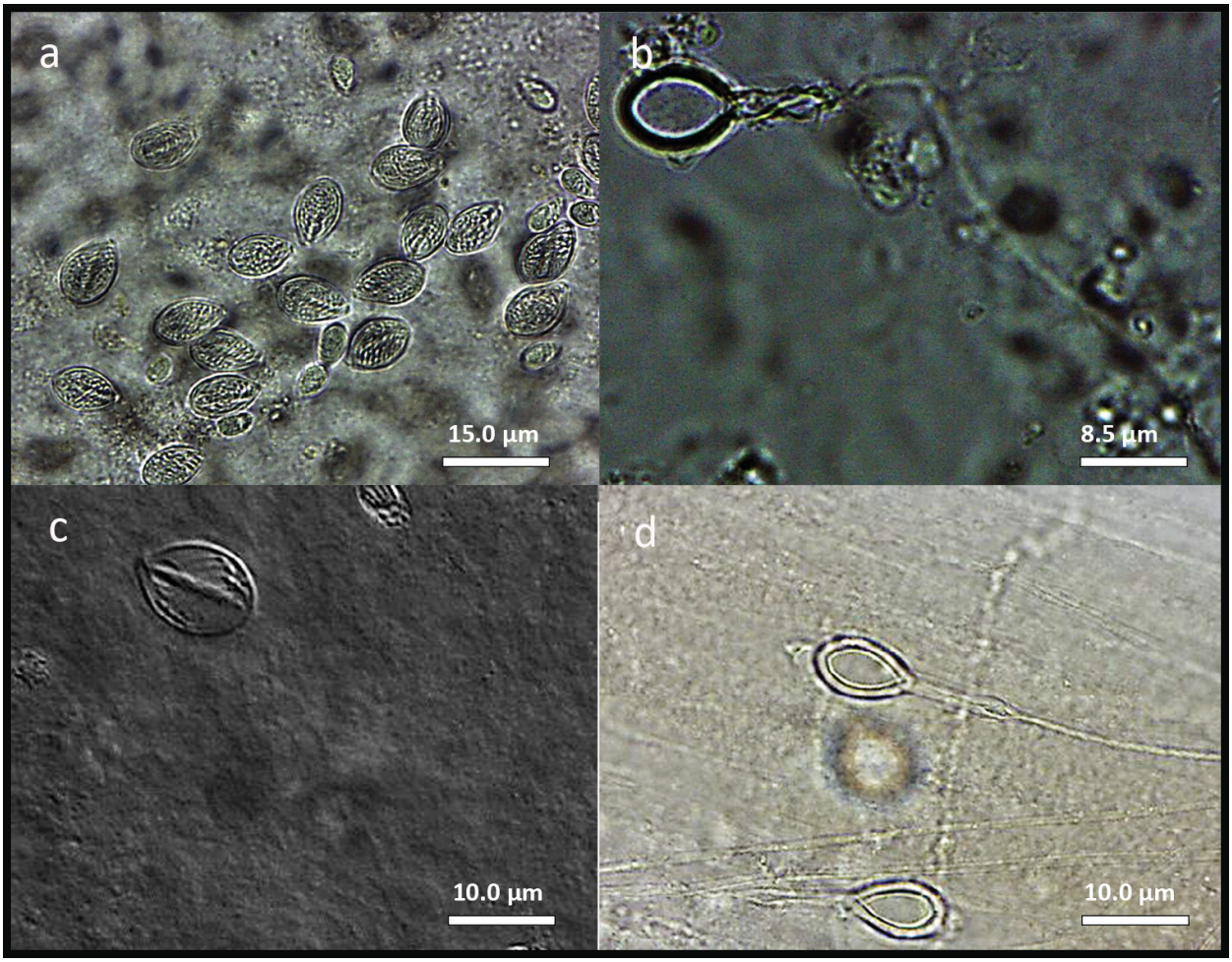

FIGURE 9. Microscopic images (1000 ×) of: a) undischarged heterotrichous microbasic bi-rhopaloids from the tentacle of *C. agulhensis* **sp. nov.**; b) discharged heterotrhichous microbasic bi-rhopaloids from the oral arm of *C. fulgida* as well as, c) undischarged microbasic euryteles from the oral arm of *C. agulhensis* **sp. nov**. and d) discharged microbasic euryteles, occurring on the oral arm of *C. fulgida.*

Type specimens. Holotype: Angola: Fish Bay: ZMB CNI 5949 (specimens ~7.5, 7.5, 9.5, and 10 cm in diameter, 10.x.1898) [damaged specimens, but in some is possible to count up to 5 tentacles per octant]

Additional material examined: 16 specimens with an umbrella diameter between 105–312 mm, collected off the coast of Namibia during March and April 2008 using a variety of sampling gears (pelagic and bottom trawls, and MOCNESS plankton nets) operated from the RV *G.O. Sars* across the area 23.33°S 14.2°E–23.67°S, 13.25°E. Five specimens have been deposited at the Iziko Museum as SAMC H5155. NNM 5361 (~17 cm in diameter, viii.1938, Walvis Bay–Namibia); USNM 53871 (as *C. quinquecirrha*, specimens ~3, 3, 5, 6, 7, 7, and 7 cm in diameter, 18.xii.1959, 4% formaldehyde solution, Ghana border, Gulf of Guinea–Togo); ZMA 2019 (as *Dactylometra fulgida*, ~17 cm in diameter, 1938, Walvis Bay–Namibia); ZMH C7452 (as *Dactylometra africana*, specimens ~10, 11, 12, and 16 cm in diameter, 29.viii.1963, Point Noire–Congo); ZMH C7451 (as *Dactylometra africana*, specimens ~14, 15, and 17 cm in diameter, no date, Point Noire–Congo), ZMUC not-numbered (as *Dactylometra quinquecirrha*, ~7 cm in diameter, 20.xii.1951, Lobito Harbour–Angola).

Type locality. Great Fish Bay, Southern Angola (16.55°S, 11.77°E)

Distribution: West coast of Africa from South Africa to the Gulf of Guinea. Coastal.

Diagnosis: *Chrysaora* of medium size, gracile. Exumbrella translucent with variable pattern of dark "purple compass" marks. Lappets and dorsal surfaces of tentacles often similarly dark-purple in colour; manubrium and oral arms without pigment, translucent, white. One primary, two secondary and two tertiary tentacles per octant, located at umbrella margin in clefts between lappets; approximately equal in length, persistent, hollow, flattened in cross-section proximally. Lappets without network of gastrovascular canals. Oral arms not spirally folded proximally.

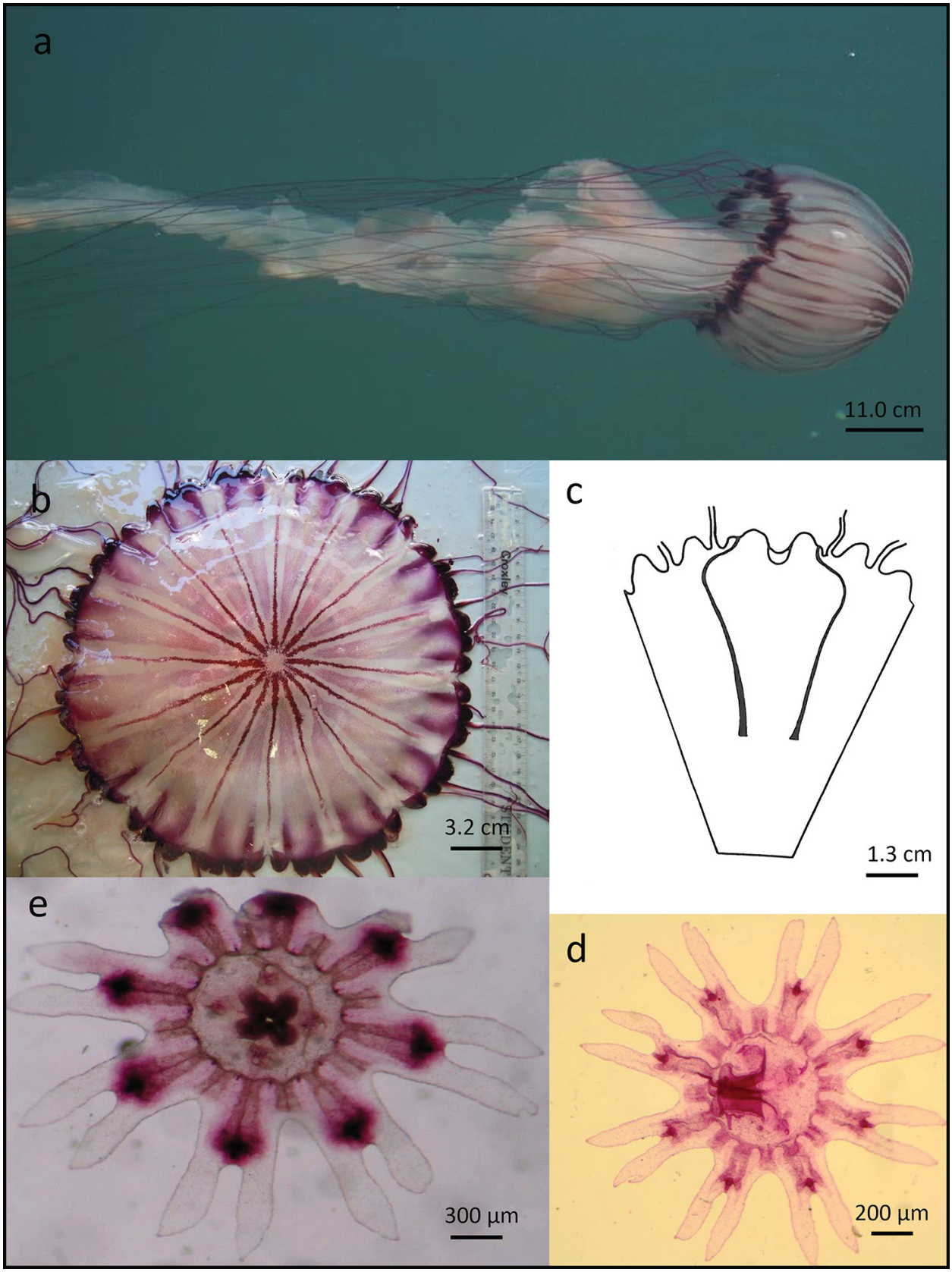

FIGURE 10. Views of *Chrysaora africana*: (a) *in situ*, (b) showing exumbrella surface and c) a graphical representation of the gastrovascular pouch shape. Wild caught ephyrae of *C. africana* from Walvis Bay, Namibia shown in d) stained with rose Bengal and e) unstained showing natural colours. Photographs with kind permission from (a) Simon Elwin, Namibian Dolphin Project and (b) Heidi Skrypzeck (Ministry of Fisheries and Marine Resources, Swakopmund).

Holotype description: Damaged specimens, in some only part remaining. Umbrella flat in preserved animals, but resembling hemispherical in shape, diameter 7.5–10 cm. Exumbrella worn out, not possible to state nematocyst warts presence, translucent cream in colour (preserved), without further markings. Umbrella slightly thickened at centre than margin. Umbrella margin damaged in all four specimens, thus total number of lappets impossible to count precisely; at least six lappets per octant: two rhopalial lappets situated next to rhopalium and four velar ones situated between rhopalial lappets. Rhopalial lappets wider than velar lappets, all with rounded edges.

Rhopalia thought to be eight situated in clefts deeper than tentacles. Rhopalium protected by sensory niche and "hood" above. Sensory pit not seen. Rhopalium itself consists of an elongated statocyst, and long, hollow, basal stem (approximately three time in length to statocyst). No ocelli observed.

Some octants with one larger primary tentacle, located in a deeper cleft, along with two well-developed secondary tentacles, sided by two tertiary tentacles (arrangement 3:2:1:2:3), for a presumed total of 40 tentacles. Tentacles laterally flattened and "ribbon-like". Radial septa arise from periphery of central stomach, dividing gastrovascular cavity into 16 pouches; septa tend to fuse at periphery of rhopalial lappets; tentacular pouches dilate distally; rhopalial pouches dilate and contract distally. Manubrium and gastrovascular pouches transparent cream in colour; manubrium arising from central stomach forms thin, tubular, slightly elongated structure with thickened mesoglea; oral opening (mouth) cruciform and situated in centre of manubrium; manubrium wall divided into four oral arms distally. Oral arms cream and translucent, with distal portion of oral arm much thinner than proximal and central portion; V-shaped in cross section; oral arms slightly spiraled; somewhat 20% longer than bell diameter. Basal portion of manubrium fused and thickened to form four gonadal pouches with four oval orifices or ostia situated between them; gonads attached to periphery of ostia and highly folded into semi-circular shape; one ostia situated between two adjacent gonads. No sperm sacs, quadralinga or gastric cirri observed.

Description of other specimens and additional data

Medusae: all dissected material was preserved; living specimens examined from photographs. In general, the preserved specimens were creamy to pale pinkish in colour: between 105–312 mm in bell diameter, gracile, roughly hemispherical in shape; exumbrella with small raised nematocyst warts. In life, exumbrella translucent, white in colour with a strongly pigmented (dark purple) pattern of (typically sixteen) alternating lines and radially distributed triangles expanding to margin: variable (Figs 10a–b). Photographs show lappets and dorsal surfaces of tentacles usually, but not always, similarly dark-purple in colour (Fig. 10b); manubrium and oral arms always without pigment, translucent, white. Umbrella thickened centrally (~6% UD in thickness), thinning towards the margin. Eight rhopalia divide the umbrella margin into octants, each comprising two rhopalial and four velar lappets; lappets roughly triangular in shape, relatively narrow (~3% UD in maximum width), becoming slightly smaller and narrower to rhopalium; rhopalial lappets indented at termination of septum, do not overlap the rhopalium; periphery of lappets free of gastrovascular canals. Rhopalium comprising a statocyst and sensory bulb, without an ocellus; situated in a deep exumbrellar pit between adjacent rhopalial lappets, cone-shaped in longitudinal cross section funnelling towards the subumbrella surface; covered by an exumbrella hood. One primary, two secondary and two tertiary tentacles per octant, located at umbrella margin in clefts between lappets; approximately equal in length, > 2x UD in length and <2% UD in width at base; persistent, hollow, flattened (not circular) in cross-section proximally. Stomach central, circular, marginally limited by sixteen radial septa; sixteen gastric pouches; septa span the entire width of the circular muscle, narrow, becoming gradually wider and strongly truncated centripetally; straight but describe pronounced curve before fusing to the edge of rhopalial lappets near base of tertiary tentacle (Fig. 10c). Manubrium surrounding a relatively broad mouth (~28% UD in width), arising as a short tube from four fairly stout (~7.5% UD in thickness) pillars proximally, distally divided into four oral arms, ~3 x UD in length. Oral arms lancet-shaped, width ~50% UD at widest point, v-shaped in cross section, highly crenulate, with delicate frills on edges; distally spiralled only (Fig. 10a). Gastric filaments in four inter-radial fields, outlined by highly folded, white/cream coloured gonads attached to the periphery of rounded sub-genital ostia: inter-ostial distance ~ half ostial length: sexes separate. Quadralinga absent.

Correlation analyses between maximum umbrella diameter and meristic as well as morphometric features were either constant (most meristic features) or significantly correlated with specimen diameter. Five standardised measures showed size dependency, including the lengths of tertiary lappets and oral arms (positive), and inter-ostial width, primary tentacle width and velar lappet length (negative): all others were size-invariant (Table 4).

Ephyrae: A single specimen collected in the Walvis Bay lagoon (22.96°S, 14.45°E); total body diameter of

2.7 mm and a central disc diameter of 1.1 mm: manubrium 306 μm in length. In life, specimen translucent with dark maroon-purple rhopalium, rhopalial canal tips and manubrium; faint rose tinge to the muscular system, velar canals, rhopalial canals and gastric filaments noted (Figs 10d–e): lacking all colour following preservation. Ephyra with 8 elongated lappet stems; with 16 non-overlapping rhopalial lappets, terminating sharply; lappet length much greater than the length of the stem. Rhopalial canals forked with rounded tips, not overtopping the rhopalium. Velar canals not forked; flat and spade-like, reaching to half the length of rhopalial canal and not extending beyond the lappet base. Gastric filament sockets were inconspicuous: one per quadrant. No marginal tentacles or tentacle bulbs observed. Conspicuous oval shaped nematocyst clusters organised in a ring like pattern around the central stomach and as pairs at the base of the marginal lappets. Cnidome of ephyrae not examined.

Cnidome: See Table 5. Relative abundances: approximately 72% of all nematocysts were heterotrichous microbasic bi-rhopaloids, about 26% were holotrichous O-isorhizas while roughly 1% was made up of atrichous isorhizas, with the abundances of nematocysts showing no distinct difference between the oral arms and tentacles. No atrichous isorhizas occurred within the tentacles.. Additionally—Nematocysts measured from tentacles of 2 specimens as presented by Morandini & Marques (2010). Specimen NNM 5361, medusa tentacles with large holotrichous O-isorhiza [n=10; 9.8–11.7 x 8.8–9.8 μm (mean = 10.78 x 9.21 μm)]; small holotrichous a-isorhizas [n=10; 5.8–6.8 x 2.9–3.9 μm (mean = 6.17 x 3.52 μm)]; holotrichous A-isorhizas [n=10; 15.6–18.6 x 8.8–11.7 μm (mean = 17.15 x 9.90 μm)]; heterotrichous microbasic rhopaloids [n=10; 10.7–13.7 x 5.8–6.8 μm (mean = 11.76 x 6.17 μm)]; Specimen ZMH C7451, medusa tentacles with medium holotrichous O-isorhizas [n=3; 10.7–12.7 x 10.7 μm (mean = 11.76 x 10.7 μm)]; large holotrichous O-isorhizas [n=10; 16.6–20.5 x 14.7–16.6 μm (mean = 19.21 x 15.78 μm)]; small holotrichous a-isorhizas [n=10; 5.8–6.8 x 2.9–3.9 μm (mean = 6.27 x 3.13 μm)]; holotrichous A-isorhizas [n=10; 15.6–19.6 x 9.8–10.7 μm (mean = 17.84 x 10.29 μm)]; heterotrichous microbasic rhopaloids [n=10; 10.7–13.7 x 6.8–7.8 μm (mean = 12.15 x 6.96 μm)]

Biological data: None available.

Genus *Chrysaora* Péron & Lesueur, 1810

Chrysaora fulgida (Reynaud, 1830)

[FIGS: 11a–b; 12a–c]

Medusa (*Rhyzostoma*) *fulgidum* Reynaud 1830: 79–80 (original description), Pl. XXV (medusa).

Chrysaora Reynaudii Lesson 1843: 401–402 (description) (the species described by Reynaud was transferred to the genus *Chrysaora* under a new name) [non *Chrysaorae Reynodii* Brandt, 1835].

Chrysaora Reynaudi: L. Agassiz 1862: 166 (mention).

Chrysaora fulgida: Haeckel 1880: 514 (description) [South Africa]. von Lendenfeld 1884: 269 (description) [False Bay–South Africa]. Vanhöffen 1888: 23 (brief description), 47 (distribution). Vanhöffen 1902: 38 (mention). Vanhöffen 1908: 39 (mention). Vanhöffen 1920: 17 (mention). Mayer 1910: 579 (synoptic table). Stiasny 1934: 388–389 (description, commented that the specimens are probably *C. hysoscella*) [Hoetjes Bay–South Africa]. Ranson 1945: 312, 316 (mention, types) [Cape of Good Hope–South Africa]. Vannucci 1954: 125 (commented that *C. fulgida* is identical to *C. hysoscella*). Kramp 1955: 296 (mention), 298 (mention, considered the synonymy *C. fulgida* = *Dactylometra africana* as doubtful). Kramp 1961: 324 (synonymy). O'Sullivan 1982: 29 (mention, = *C. africana*). Pagès, Gili & Bouillon 1992: 50 (mention). Gershwin & Collins 2002: 128 (mentioned as nominal species with insufficient data).

Chrysaora hysoscella var. *fulgida* Mayer 1910: 581 (brief description). Pagès, Gili & Bouillon 1992: 50 (mention) [non *Chrysaora hysoscella* (Linnaeus, 1767)].

Dactylometra quinquecirrha: Stiasny 1931: 139 (mention) [Lagos–Nigeria] [non *Chrysaora quinquecirrha* (Desor, 1848)].

Dactylometra fulgida: Stiasny 1939: 172–173 (description), 173–184 (discussion, probably the *Chrysaora* stage of *D. africana*), fig. 1 (medusa, reproduction of the original figure) [South Africa].

?*Chrysaora quinquecirrha*: Kramp 1955: 297–300 (description, *D. africana* = *D. quinquecirrha*, comments on differences with *C. lactea*, comparison of nematocysts with *C. hysoscella*), 305 (ephyrae), 309 (mention), 314 (tab. III), 317 (mention) [Angola; Nigeria]. Mianzan & Cornelius 1999: 538 (description), fig. 2.17 (distribution), figs 5.14a– b (medusa) [eastern Atlantic Ocean, Africa] [non *Chrysaora quinquecirrha* (Desor, 1848)].

Type specimens: HOLOTYPE

Examined material: 40 specimens with an umbrella diameter between 59–407 mm, collected off the coast of Namibia during March and April 2008 using a variety of sampling gears (pelagic and bottom trawls, and MOC-

NESS plankton nets) operated from the RV *G.O. Sars* across the area 23.33°S 14.2°E–23.67°S, 13.25°E: Three ephyrae (MB-A088461) and polyps obtained following the settlement of planulae from specimens of *Chrysaora fulgida* originally collected from Walvis Bay (22.93°S, 14.45°E) in 2012. Nine specimens have been deposited at the Iziko Museum, Cape Town, as SAMC H5156.

Type locality: Cape of Good Hope, South Africa.

Diagnosis: *Chrysaora* of large size, robust. Exumbrella rose/orange colour with variable pattern of darker brown compass marks. Lappets pigmented; oral arms deep orange and highly spiralled/ convoluted. One primary and two secondary per octant, located at umbrella margin in clefts between lappets; approximately equal in length, not persistent and cylindrical: maroon in colour. Lappets with network of gastrovascular canals. Oral arms lavishly spiralled basally.

Holotype description (From Morandini and Marques 2010): "Umbrella less than a hemisphere, ~8.5 cm in diameter. Exumbrellar surface finely granulated. Mesoglea flexible, thicker centrally. Marginal lappets 4 per octant (2 rhopalar, 2 tentacular), rounded; without canals of gastrovascular system; rhopalar lappets not overlapping ("open rhopalia" condition). Rhopalia 8, without ocelli, in deep clefts; exumbrellar sensory pit deep. Tentacular clefts vary in depth. Tentacles 24 (3 per octant), as long as bell diameter, arranged as 2nd-1st-2nd (primary tentacle central, secondary tentacles laterally). Subumbrellar musculature not distinguishable. Brachial disc circular, with 4 evident corners. Pillars evident, 2 cm wide, delimited by insertion corners of manubrium. Subgenital ostia rounded, 0.7 cm in diameter. Oral arms *ca.* bell diameter long, V-shaped. Central stomach circular, marginal region limited by insertion of radial septa. Stomach pouches 16, width uniform centrally; tentacular pouches enlarged distally. Radial septa narrow, at proximal end wider, pear-shaped; outer 1/3 bending towards rhopalia (~45º); ending near tentacular base at rhopalar lappet. Gastric filaments not observed. Quadralinga absent. Gonads semicircular ring, greatly folded; sex not determined".

Description of other specimens and additional data

Medusae: Medusae massive, up to 80 cm in diameter and 20 kg in weight (unpublished data), roughly hemispherical in shape; exumbrella smooth, lacking raised nematocyst warts. Exumbrella of small (<8 cm UD) specimens lacking pigmentation, translucent pink in colour; oral arms pink/white (Fig. 11a). Exumbrella of large specimens otherwise translucent rose-red-orange in colour; frills on oral arms orange/brown, inner portion of oral arms opaque and colourless; marginal tentacles deep maroon. Exumbrella with characteristic star-shaped pattern formed from (typically) sixteen, darker-than-base pigmented, radially distributed triangles expanding to margin (Fig. 11b). Umbrella thickened centrally (~18% umbrella diameter (UD) in thickness), thinning to margin. Eight rhopalia divide the umbrella margin into octants, each comprising two rhopalial and no more than two velar lappets; lappets broad (~8.5% UD in width) and flat, semi-circular; rhopalial lappets slightly more rounded than velar lappets, do not overlap the rhopalium; gastrovascular canals project as branching finger-like network into base (but not periphery) of lappets. Rhopalia as in *C. agulhensis* **sp. nov.**, but with a thickened endoderm that extends outwards for a relatively long distance (0.3 times the length of the rhopaliar canal) (Appendix 3) along the sides of the lappets. The rhopalium itself consists of a statocyst and a short, hollow, basal stem that is 1.5 times the length of the statocyst (Appendix 3), which is clasped by a subumbrellar bulb and receives the rhopalar canal, which is approximately twice as long as the statocyst. No ocelli observed. Eight persistent and prominent primary tentacles, one per octant, located at umbrella margin in deepish clefts between velar lappets, <2 x UD in length and ~2.3% UD in width at base; up to two deciduous secondary tentacles per octant, half width of primary tentacles at base, located in shallow clefts between rhopalial and velar lappets: hollow, circular in cross-section. Tentacles maroon in colour. Stomach central, circular, marginally limited by sixteen radial septa; sixteen gastric pouches; septa span the entire width of the circular muscle, narrow, rounded centripetally; straight but describe pronounced curve before fusing to the edge of rhopalial lappets near mid-line (Fig. 11d). Manubrium surrounding relatively small mouth (~18% UD), arising as a short, thin tube from four relatively thin (~5% UD in thickness) pillars proximally, distally divided into four oral arms, approximately 2 x UD in length. Oral arms lancet-shaped, width ~ 40% UD at widest point, distally spiralled; v-shaped in cross section, highly crenulate, with delicate frills on edges; spiral. Gastric filaments in four interradial fields, outlined by highly folded gonads suspended from sub-umbrella surface in thin membranous sacs, protrude through relatively narrow (~6% UD) and rounded sub-genital ostia: inter-ostial distance approximately equal to ostial length: microscopic examination of gonads indicates sexes gonochoric. Quadralinga present in large specimens i.e. >40 cm UD; sperm sacs absent.

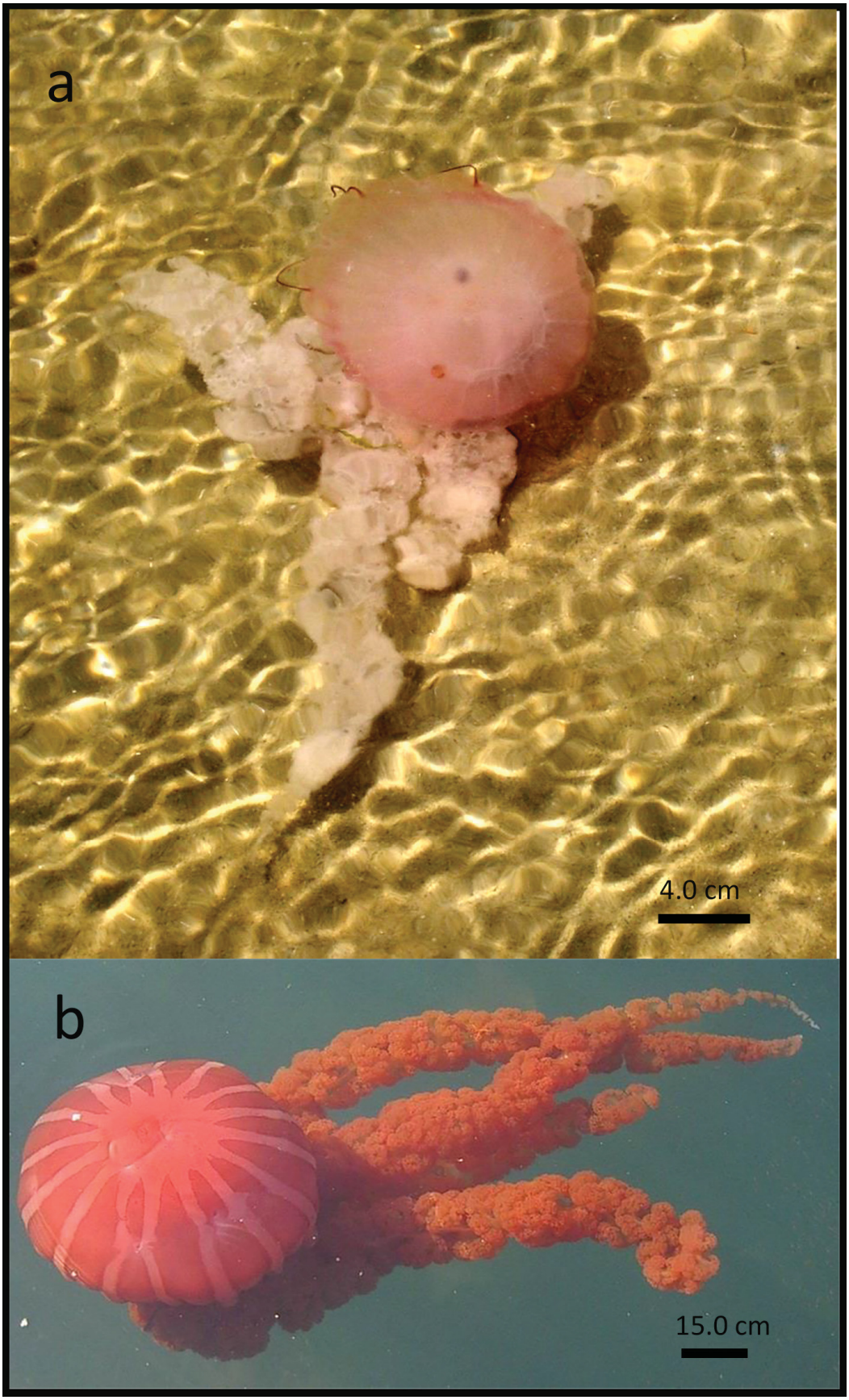

FIGURE 11. Photographs of live *Chrysaora fulgida* in the northern Benguela ecosystem, illustrating colour pattern variation between a) juvenile medusae and, b) adult medusa. Highly folded oral arms are clearly represented in b. Photographs with kind permission from Simone Neethling, The University of the Western Cape.

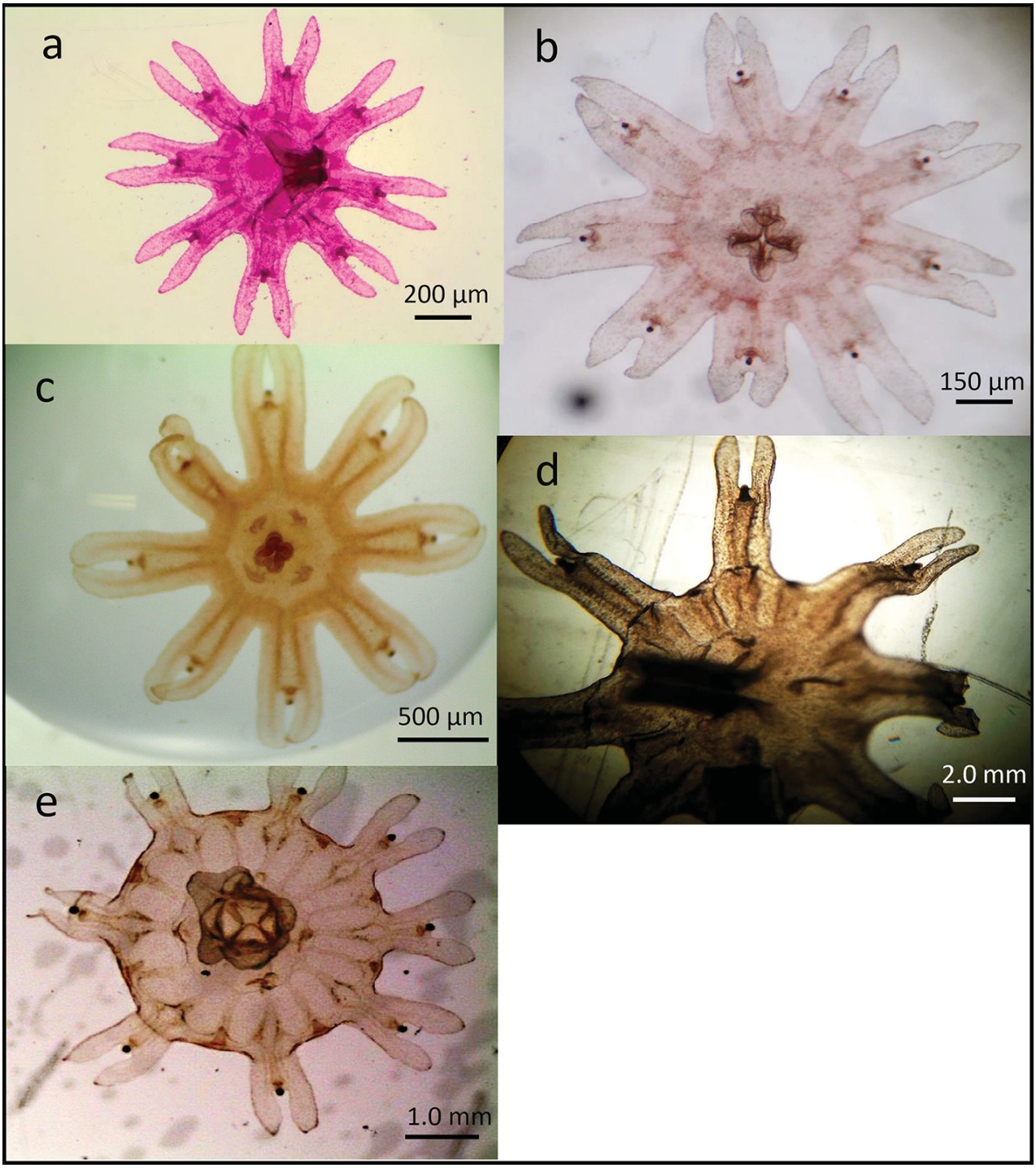

FIGURE 12. Enlarged images of the ephyrae of *C. fulgida*: a) wild caught ephyrae stained with rose Bengal, b) wild caught ephyrae, unstained showing natural colours. Cultured ephyrae, unfed, at c) two days post liberation, d) two weeks post liberation and e) 30 days post liberation. Lappets stems, lappets, nematocyst clusters and gastric filaments clearly visible.

In preservation, small specimens generally cream in colour; tentacles orange-brown, while large specimens generally orange-brown in colour with/without darkly pigmented radial patterns; gonads and inner portion of oral arms and manubrium cream.

There is a high degree of variation in the radial patterning on the exumbrella: some specimens lack the darkly pigmented central apex, others lack well defined triangles. One specimen possessed nine rhopalia. Correlation analyses between umbrella diameter and meristic and morphometric features were either constant (most meristic features) or significantly correlated with specimen diameter. Only three standardised measures showed a significant

relationship (negative) with size: mouth diameter, and ostial width and length (Table 4). Quadralinga noticeably present only in the largest specimens, suggesting they may have a supportive and structural function. This could also suggest qaudralinga to be present in smaller specimens but perhaps not noticeably so.

Polyp: Polyps of *C. fulgida* were reared from material collected in the Walvis Bay lagoon (22.92°S, 14.47°E). Typically, conical in shape, up to 4 mm in height (Appendix 3). Oral disk roughly half the length of the polyp. Usually possesses 16 tentacles, up to four times the length of the polyp height (Appendix 3); with four gastric septa and a cruciform mouth. Pale peach in colour unless strobilating, in which case the upper half becomes brown.

Ephyrae: Wild caught Stage-0 ephyrae with total body diameter of 2.1 mm ± 480.94 μm and a central disc diameter of 0.96 mm ± 289.09 μm. The manubrium was ~317.00 ± 160.75 μm in length. Live specimens peach to pale pink in colour; colourless once preserved. With 8 elongated lappet stems, and 16 indistinctly pointed, non-overlapping rhopalial lappets; lappet length slightly greater than the length of the stem (Appendix 3); rhopalial canals forked with rounded tips, not reaching beyond rhopalial niche base (Figs 12a–b). Velar canals slightly forked with rounded tips, reaching only to lower third of the rhopalial canals. Four gastric filament sockets, with between 0 to 1 gastric filaments each. No marginal tentacles or tentacle bulbs observed. Nematocyst clusters inconspicuous and difficult to observe: at base of lappets, along the rhopalial canals and scattered throughout the central disk (Figs 12a–b). Laboratory reared ephyrae similar at one to 14-days (stage 0) (Figs 12c–e), with total body diameter of 2.1 mm ± 400.17 μm, a central disk diameter of 0.93 ± 225.1 μm, with manubrium 700 ± 212.32 μm in length. However, post liberation: may possess a single tentacle bud, situated in between lappet stems. Manubrium prominent, relatively narrow but long, approximately 30 % of the central disk diameter (Appendix 3). Nematocysts: Approximately 65% of all nematocysts found within the ephyrae were Holotrichous O-isorhizas (L = 10.2 ± 0.25 μm; W = 8.8 ± 0.25 μm), while the remaining 35% constituted heterotrichous microbasic bi-rhopaloids (L = 9.9 ± 0.18; W = 8.4 ± 0.27 μm).

Cnidome: See Table 5 for individual measures. Relative abundances: the proportions of heterotrichous microbasic bi-rhopaloids, differed between the oral arms and tentacles, with the oral arms containing approximately 63% bi-rhopaloids while the tentacles contained roughly 34% bi-rhopaloids. Similarly, the oral arms contained approximately 29% holotrichous O-isorhizas while roughly 47% of nematocysts within the tentacles were holotrichous O-isorhizas. The oral arms also possessed a lower abundance of holotrichous A-isorhizas (8%) than the tentacles (18%) and less than 1% consisted of a*trichous isorhizas.* The tentacles possessed a higher abundance of nematocysts overall. Additionally, From Morandini and Marques (2010)—Specimen **NNM 5361**, medusa tentacles with large holotrichous O-isorhiza [n=10; 9.8–11.7 x 8.8–9.8 μm (mean = 10.78 x 9.21 μm)]; small holotrichous a-isorhizas [n=10; 5.8–6.8 x 2.9–3.9 μm (mean = 6.17 x 3.52 μm)]; holotrichous A-isorhizas [n=10; 15.6–18.6 x 8.8–11.7 μm (mean = 17.15 x 9.90 μm)]; heterotrichous microbasic rhopaloids [n=10; 10.7–13.7 x 5.8–6.8 μm (mean = 11.76 x 6.17 μm)]; Specimen **ZMH C7451**, medusa tentacles with medium holotrichous O-isorhizas [n=3; 10.7–12.7 x 10.7 μm (mean = 11.76 x 10.7 μm)]; large holotrichous O-isorhizas [n=10; 16.6–20.5 x 14.7–16.6 μm (mean = 19.21 x 15.78 μm)]; small holotrichous a-isorhizas [n=10; 5.8–6.8 x 2.9–3.9 μm (mean = 6.27 x 3.13 μm)]; holotrichous A-isorhizas [n=10; 15.6–19.6 x 9.8–10.7 μm (mean = 17.84 x 10.29 μm)]; heterotrichous microbasic rhopaloids [n=10; 10.7–13.7 x 6.8–7.8 μm (mean = 12.15 x 6.96 μm)].

Remarks. The taxonomic history of *Chrysaora africana* exemplifies the problems of species identity within this genus, based, as it has been, on generally vague and markedly incomplete original descriptions. *Dactylometra africana* was originally described by Vanhöffen (1902) from material collected on a regional survey from Southern Angola as having 40 tentacles and 48 lappets. He also noted the strong purple colour of exumbrella markings. In that same survey, Vanhöffen (1902) also caught two damaged specimens of *Chrysaora* from Algoa Bay along the South coast of South Africa, which he recognised as distinct from *D. africana*, and which he tentatively considered might be *C. fulgida,* though he described them as *Chrysaora* sp. Whilst the validity of *D. africana* was upheld by Mayer (1910), Stiasny (1939) disagreed; describing five *Chrysaora* medusae with 48 lappets from Walvis Bay (Namibia) as *C. fulgida* and not *C. africana.* His arguments for synonymising the two were based almost entirely on the patterns and colour (brown not red) of markings on the exumbrella, and on the assumption that these scyphozoans underwent a progressive development according to lappet (and tentacle) number: a sexually mature 32 lappets (24 tentacle) *C. fulgida* developing into a 48 lappet (40 tentacle) *C. africana*, the latter representing the "dactylometra" stage of the former. While a number of authors failed to be fully convinced by Stiasny's (1939) arguments (e.g. Ranson 1949; Kramp 1955, 1961), the recent literature suggests otherwise (e.g. Pagès *et al.* 1992; Mianzan & Cornelius 1999; Morandini & Marques 2010). Colour patterns are notoriously variable (Morandini & Marques 2010), especially in

C. africana, and they are subject to artefacts induced by preservation. Unlike Vanhöffen's (1902) original description, which was based on fresh material, that of Stiasny (1939) was based on preserved specimens that had been sent to him by "Dr Engel". Our own observations indicate (above) that the purple colour of living specimens fades to red/brown on preservation. Even small specimens of *C. africana* possess 48 lappets and 40 marginal tentacles and are strongly pigmented; all specimens of *C. fulgida,* possess 32 lappets and (up to) 24 tentacles and the species gets much bigger than *C. africana*.

The resurrection of *C. africana* from *C. fulgida* as first argued by Neethling (2010) is mirrored by Bayha *et al.*'s (2017) resurrection of *C. chesapeakei* from *C. quinquicirrha*. In the former case, a 40 tentacle species had been synonymised with a 24 tentacle species, whilst in the latter case, a 24 tentacle species had been synonymised with a 40 tentacle species. There are other interesting parallels between the two sympatric taxa. The two 40 tentacle species (*C. africana* and *C. quinquicirrha*) both enjoy relatively wide distributions on their respective sides of the Atlantic that extend into subtropical waters. By contrast, the two 24 tentacle species (*C. fulgida* and *C. chesapeakei*) enjoy more coastal distributions and are relatively restricted in geographic extent. The two 40 tentacle species have relatively simple oral arms, whilst the two 24 tentacle species have densely spiralled and "lush" oral arms. Bayha *et al.* (2017), building on arguments presented by Bayha & Dawson (2010), suggested that this is an adaptation to feeding extensively on gelatinous prey items, which in the case of *C. chesapeakei*, could be the ctenophore *Mnemiopsis leidyi* (Feigenbaum & Kelly 1984; Bayha *et al.* 2017; Bologna *et al.* 2017). The only other common gelatinous species found within the range typically occupied by *C. fulgida* is the hydromedusa *Aequorea forskalia* (Sparks *et al.* 2001). Of the two, the latter is more numerous than the former off coastal Namibia (Lynam *et al.* 2006), but it is distributed offshoreward of *C. fulgida*. Indeed, there is a strongly negative relationship between the distribution and abundance of the two species, which Sparks *et al.* (2001) suggested could be a result of intraguild predation. A hypothesis reinforced by the comments of Bayha *et al.* (2017).

There are two other Atlantic species of *Chrysaora* with 48 lappets (and 40 tentacles): *C. quinquecirrha* in the NW and *C. lactea* in the SW. Vanhöffen (1902) recognised a similarity between *C. africana* and the former, and Kramp (1955) and Mianzan & Cornelius (1999) synonymised the two. *Chrysaora quinquecirrha* can be separated from *C. africana,* however, by its closed rhopalial condition, by the form of the radial septa (pear-shaped proximally and not strongly truncated), and by the fact that the tertiary tentacles are usually much smaller than the others and they arise from beneath the rhopalial lappet (Morandini & Marques 2010). Like *C. africana, C. quinquecirrha* is generally pale in colour but tentacles and other highly pigmented areas are usually orange/ochre in colour and never deep-purple. *Chrysaora lactea* may also have five tentacles per octant, but can be separated from *C. africana* by the comparatively shorter length of the oral arms, the lack of strongly pigmented tentacles and differences in the form of the radial septa (strongly pear-shaped, not truncated, proximally).

Morphological and molecular evidence show that there are three species of *Chrysaora* in the waters off the west coast of southern Africa. The three species can be readily distinguished in the field through morphological features described in Table 10. Of the three species, *C. fulgida* is the more abundant and is often caught over the shelf off Namibia. It is also the species that was responsible for the shutdown of the Koeberg nuclear power plant in autumn 2005 off the west coast of South Africa (Maposa 2005). *C. fulgida* is the local species that has been uncritically referred to as *C. hysoscella* (following Pagés *et al.* 1992) in the literature to date (e.g. Venter 1988; Fearon *et al.* 1992; Brierley *et al.* 2001; Buecher *et al.* 2001; Mills 2001; Sparks *et al.* 2001; Brierley *et al.* 2004; Lynam *et al.* 2006; Flynn & Gibbons 2007; Purcell *et al.* 2007; Palomares & Pauly 2009). It is a shelf species that reaches greatest abundance inshore of the 200 m depth contour, and appears to be restricted to the waters of the Benguela upwelling ecosystem. *Chrysaora africana*, by contrast, is relatively uncommon in the region and its populations are not known to reach high levels of abundance. As a consequence, this species has not been subject to ecological study. That said, it is more widely distributed than *C. fulgida* in the SE Atlantic and can be found from False Bay (unpublished observations) on the South African SW coast to Guinea-Bissau on the bulge of West Africa (Ranson 1949). *Chrysaora agulhensis* **sp. nov.** is essentially an Agulhas Bank endemic, with reported sightings stretching from Table Bay eastwards to Algoa Bay (Sink *et al.* 2017).

Whilst there are gaps in the present morphological descriptions, and we have provided no description of the polyps of *Chrysaora africana* (as Morandini & Marques 2010), our data have nevertheless shown that the use of multiple lines of evidence is important in delineating species. That said, behavioural and ecological studies should also be undertaken in an attempt to better understand all the species and their possible origin. Using a holistic approach such as the one employed in this study, may also potentially be the key in better resolving schyphozoan taxonomy

and particularly that of the *Chrysaora*. A shift from single gene regions to whole genome sequencing may also be required to more unambiguously differentiate between closely related and congeneric species.

TABLE 10. Morphological features that allow easy separation of *Chrysaora fulgida*, *C. africana* and *C. agulhensis* **sp. nov.** in the field.

Features	*C. africana*	*C. fulgida*	*C. agulhensis* sp. nov.
Bell colour	translucent-white with purple stripes	orange-brown	purple
Bell pattern	star-shaped	sometimes star-shaped	always star-shaped
Oral arms	translucent white	orange to deep red	purple
Number of lappets	48	32	32
Number of rhopalia	8	8	8
Tentacle shape	cylindrical	cylindrical	laterally flattened
Tentacle colour	purple	white	cream
Number of tentacles	40	24	24
Gonads	attached to periphery of four rounded subgenital ostia	situated in central stomach, attached to subumbrellar surface	situated in central stomach, attached to subumbrellar surface

Acknowledgements

We would like to thank Dr Deborah Robertson-Andersson (University of KwaZulu Natal, South Africa), and Mr Krish Lewis (Two Oceans Aquarium, South Africa), as well as the officers and crew of the R.V. *G.O. Sars,* for their assistance in the collection of material. We are grateful to the staff at the national natural history museums in London, Paris and Berlin for giving us access to preserved specimens of *Chrysaora hysoscella,* and to Type specimens of *C. fulgida* and *C. africana,* respectively. To Prof Tom Doyle (NUI Galway, Ireland), thanks for collecting genetic material of *Chrysaora hysoscella.* We are grateful to Martin Hendricks and Alan Channing (UWC) for technical support and to Hannelore Van Ryneveld (UWC) and Bruno Viertel (Univ. Mainz) for assistance in translating old German. Particular thanks are also due to Mike Dawson and Liza Gómez-Daglio for their useful comments on earlier drafts of the manuscript. This work was supported by the National Research Foundation, the NRF-Royal Society (London) SET Development grant in Zoology to the University of the Western Cape; and the Canon Collins Trust (S.N., grant number Nee 1500).

Author Contributions

MJG conceptualized project. VR and SN performed morphological measurements on all species. MJG and VR performed statistical analyses on morphological data. VR performed all wet lab work and data analysis for genetic data. KMB and ACE provided supervision and assistance on genetic analyses. ACM provided descriptions for museum holotypes and HS provided photographs and descriptions of wild ephyrae. All authors contributed to writing and reviewing the manuscript.

References

Abboud, S.S, Gómez Daglio, L. & Dawson, M.N. (2018) A global estimate of genetic and geographic differentiation in macromedusae—implications for identifying the causes of jellyfish blooms. *Marine Ecology Progress Series*, 591, 199–216. https://doi.org/10.3354/meps12521

Agassiz, L. (1862) *Contributions to the Natural History of the United States of America*. *Vol. IV. Pt. III. Discophorae. Pt. IV. Hydroidae. Pt. V. Homologies of the Radiata*. Little Brown Trubner, Boston, London, 380 pp.

Akaike, H. (1973) Information theory and an extension of the maximum likelihood principle. *In*: Petrov, P.N. & Csaki, F. (Eds.), *Second International Symposium on Information Theory*. Adad. Kiado, Budapest, pp. 267–281.

Anderson, M.J., Gorley, R.N. & Clarke, K.R. (2008) *PERMANOVA+ for PRIMER: Guide to Software and Statistical Methods*. PRIMER-E, Plymouth, 214 pp.

Awad, A.A., Griffiths, C.L. & Turpie, J.K. (2002) Distribution of South African marine invertebrates applied to the selection of priority conservation areas. *Diversity & Distribution*, 8, 129–145. https://doi.org/10.1046/j.1472-4642.2002.00132.x

Bayha, K.M., Collins, A.G. & Gaffney, P.M. (2017) Multigene phylogeny of the scyphozoan jellyfish family Pelagiidae reveals that the common U.S. Atlantic sea nettle comprises two distinct species (*Chrysaora quinquecirrha* and *C. chesapeakei*) *PeerJ*, 5, e3863. https://doi.org/10.7717/peerj.3863

Bayha, K.M., Dawson, M.N., Collins, A.G., Barbeitos, M.S. & Haddock, S.H.D. (2010) Evolutionary relationships among scyphozoan jellyfish families based on complete taxon sampling and phylogenetic analysis of 18S and 28S ribosomal DNA. *Integrative and Comparative Biology*, 50 (3), 436–455. https://doi.org/10.1093/icb/icq074

Bologna, P., Gaynor, J.J., Meredith, R., Restaino, D. & Barry, C. (2018) Stochastic event alters gelatinous zooplankton community structure: impacts of Hurricane Sandy in a Mid-Atlantic estuary. *Marine Ecology Progress Series*, 591, 217−227. https://doi.org/10.3354/meps12262

Brierley, A.S., Axelsen, B.E., Buecher, E., Sparks, C., Boyer, H. & Gibbons, M.J. (2001) Acoustic observations of jellyfish in the Namibian Benguela. *Marine Ecology Progress Series*, 210, 55–66. https://doi.org/10.3354/meps210055

Brierley, A.S., Axelsen, B.E., Boyer, D.C., Lynam, C.P., Didcock, C.A., Boyer, H.J., Sparks, C.A.J., Purcell, J.E. & Gibbons, M.J. (2004) Single-target echo detections of jellyfish. *ICES Journal of Marine Science*, 61, 383–393. https://doi.org/10.1016/j.icesjms.2003.12.008

Brodeur, R.D., Link, J.S., Smith, B.E., Ford, M., Kobayashi, D. & Jones, T.T. (2016) Ecological and economic consequences of ignoring jellyfish:a plea for increased monitoring of ecosystems. *Fisheries*, 41, 630−637. https://doi.org/10.1080/03632415.2016.1232964

Buecher, E., Sparks, C., Brierley, A., Boyer, H. & Gibbons, M.J. (2001) Biometry and size distribution of *Chrysaora hysoscella* (Cnidaria, Scyphozoa) and *Aequorea aequorea* (Cnidaria, Hydrozoa) off Namibia with some notes on their parasite *Hyperia medusarum*. *Journal of Plankton Research*, 23, 1073–1080. https://doi.org/10.1093/plankt/23.10.1073

Carlgren, O. (1940) A contribution to the knowledge of the structure and distribution of the cnidae in Anthozoa. *Lunds Universitet´s Årskrift*, 36, 1–62.

Darriba, D., Taboada, GL., Doallo, R. & Posada, D. (2012) jModelTest 2: more models, new heuristics and parallel computing. *Nature Methods*, 9, 772. https://doi.org/10.1038/nmeth.2109

Dawson, M.N. (2003) Macro-morphological variation among cryptic species of the moon jellyfish, *Aurelia* (Cnidaria: Scyphozoa). *Marine Biology*, 143, 369–379. https://doi.org/10.1007/s00227-003-1070-3

Dawson, M.N. (2005) Morphological variation and systematics in the Scyphozoa: *Mastigias* (Rhizostomeae, Mastigiidae)—a golden unstandard? *Hydrobiologia*, 537, 185–206. https://doi.org/10.1007/s10750-004-2840-8

Dawson, M.N. & Jacobs, D.K. (2001) Molecular evidence for cryptic species of *Aurelia aurita* (Cnidaria, Scyphozoa). *Biological Bulletin*, 200, 92–96. https://doi.org/10.2307/1543089

de Lafontaine, Y. & Leggett, W.C. (1989) Changes in size and weight of hydromedusae during formalin preservation. *Bulletin of Marine Science*, 44, 1129–1137.

Desor, E. (1848) No title. Meeting of the November 1, 1848. *Proceedings of the Boston Society of Natural History*, 3 (1848–1851), 73–77. [Desor part, pp. 75–76.] https://doi.org/10.1080/03745485809494477

Dwivedi, B. & Gadagkar, S.R. (2009) Phylogenetic inference under varying proportions of indel-induced alignment gaps. *BMC Evolutionary Biology*, 9, 211. https://doi.org/10.1186/1471-2148-9-211

Fearon, J.J., Boyd, A.J. & Schülein, F.H. (1992) Views on the biomass and distribution of *Chrysaora hysoscella* (Linné) and *Aequorea aequorea* (Forskål, 1775) off Namibia 1982–1989. *Scientia Marina*, 56, 75–85.

Feigenbaum, D.L. & Kelly, M. (1984) Changes in the lower Chesapeake Bay food chain in the presence of the sea nettle *Chrysaora quinquecirrha* (Scyphomedusae). *Marine Ecology Progress Series*, 19, 39–47 https://doi.org/10.3354/meps019039

Felsenstein, J. (1985) Confidence limits on phylogenies: An approach using the bootstrap. *Evolution*, 39, 783–791 https://doi.org/10.1111/j.1558-5646.1985.tb00420.x

Flynn, B.A. & Gibbons, M.J. (2007) A note on the diet and feeding of *Chrysaora hysoscella* in Walvis Bay Lagoon, Namibia, during September 2003. *African Journal of Marine Science*, 29, 303–307. https://doi.org/10.2989/ajms.2007.29.2.15.197

Folmer, O., Black, M., Hoeh, W., Lutz, R. & Vrijenhoek, R. (1994) DNA primers for amplification of mitochondrial cytochrome *c* oxidase subunit I from diverse metazoan invertebrates. *Molecular Marine Biology and Biotechnology*, 3, 294–299.
Gegenbaur, C. (1856) Versuch eines Systemes der Medusen, mit Beschreibung neuer oder wenig gekannter Formen; zugleich ein Beitrag zur Kenntnis der Fauna des Mittelmeeres. *Zeitschrift für Wissenschaftliche Zoologie, Leipzig*, 8, 202–273.
Gershwin, L. & Collins, A.G. (2002) A preliminary phylogeny of Pelagiidae (Cnidaria, Scyphozoa), with new observations of *Chrysaora colorata* comb. nov. *Journal of Natural History*, 36, 127–148.
https://doi.org/10.1080/00222930010003819
Gómez-Daglio, L. (2016) Systematics and phylogeny of shallow water jellyfish (Scyphozoa, Discomedusae in the Tropical Eastern Pacific. PhD thesis. Accessible from: https://escholarship.org/uc/item/03s3r0qf (accessed 23 March 2013)
Gómez-Daglio, L. & Dawson, M.N. (2017) Species richness of jellyfishes (Scyphozoa:Discomedusae) in the Tropical Eastern Pacific: missed taxa, molecules, and morphology match in a biodiversity hotspot. *Invertebrate Systematics*, 31, 635−663.
https://doi.org/10.1071/IS16055
Griffiths, C.L., Robinson, T.B., Lange, L. & Mead, A. (2010) Marine biodiversity in South Africa–state of knowledge, spatial patterns and threats. *PLoS ONE*, 5 (8), e123008.
https://doi.org/10.1371/journal.pone.0012008
Hall, T. (2005) BioEdit, Biological sequence alignment editor for Win95/98/NT/2K/XP. Available from: www.mbio.ncsu.edu/BioEdit/bioedit.html. (accessed 23 March 2013)
Haeckel, E. (1880) 2: System der Acraspeden. *In*: *Das System der Medusen. I.* Gustav Fischer, Jena, pp. 361–672.
Holland, B., Dawson, M., Crow, G. & Hofmann, D. (2004) Global phylogeography of *Cassiopea* (Scyphozoa: Rhizostomeae): molecular evidence for cryptic species and multiple invasions of the Hawaiian Islands. *Marine Biology*, 145, 1119–1128.
https://doi.org/10.1007/s00227-004-1409-4
Hutchings, L., Barange, M., Bloomer, S.F., Boyd, A.J., Crawford, R.J.M., Huggett, J.A., Kerstan, M., Korrûbel, J.L., de Oliveira, J.A.A., Painting, S.J., Richardson, A.J., Schülein, F.H., van der Lingen, C.D. & Verheye, H.M. (1998) Multiple factors affecting South African anchovy recruitment in the spawning, transport and nursery areas. *South African Journal of Marine Science*, 19 (1), 211–225.
https://doi.org/10.2989/025776198784126908
Hutchings, L., Van der Lingen, C.D., Shannon, L.J., Crawford, R.J.M., Verheye, H.M.S., Bartholomae, C.H., Van der Plas, A.K., Louw, D., Kreiner, A., Ostrowski, M., Fidel, Q., Barlow, R.G., Lamont, T., Coetzee, J., Shillington, F., Veitch, J., Currie, J.C. & Monteiro, P.M.S. (2009) The Benguela Current: an ecosystem of four components. *Progress in Oceanography*, 83 (1–4), 15–32.
https://doi.org/10.1016/j.pocean.2009.07.046
Kramp, P.L. (1955) The medusae of the tropical west coast of Africa. *Atlantide Reports*, 3, 239–324.
Kramp, P.L. (1961) Synopsis of the medusae of the world. *Journal of Marine Biological Association of the United Kingdom*, 40, 1–469.
https://doi.org/10.1017/s0025315400007347
Kumar, S., Stecher, G., Li, M., Knyaz, C. & Tamura, K. (2018) MEGA X: Molecular Evolutionary Genetics Analysis across computing platforms. *Molecular Biology and Evolution*, 35, 1547–1549.
https://doi.org/10.1093/molbev/msy096
Lesson, R.P. (1843) *Histoire naturelle des Zoophytes, Acalèphes*. Librairie Encyclopédique de Roret, Paris, 596 pp.
https://doi.org/10.5962/bhl.title.4799
Linnaeus, C. (1767) *Systema naturae per regna tria naturae: secundum classes, ordines, genera, species cum characteribus, differentiis, sinonimis, locis. Editio duodecima, reformata. Tomus I. Pars II*. Laurentii Salvii, Holmiae, 550 pp.
https://doi.org/10.5962/bhl.title.158187
Lucas, C.H. (2009) Biochemical composition of the mesopelagic coronate jellyfish *Periphylla periphylla* from the Gulf of Mexico. *Journal of the Marine Biological Association of the United Kingdom*, 89, 77–81
https://doi.org/10.1017/S0025315408002804
Lucas, C.H., Graham, W.M. & Widmer, C. (2012) Jellyfish life histories: role of polyps in forming and maintaining scyphomedusa populations. *Advances in Marine Biology*, 63, 133−196.
https://doi.org/10.1016/B978-0-12-394282-1.00003-X
Lutjeharms, J.R.E. & Cooper, J. (1996) Inter-basin leakage through Agulhas Current filaments. *Deep-Sea Research*, 43, 213–238
. https://doi.org/10.1016/0967-0637(96)00002-7
Lynam, C.P., Gibbons, M.J., Axelsen, B.A., Sparks, C.A.J., Coetzee, J., Heywood, B.G. & Brierley, A.S. (2006) Jellyfish overtake fish in a heavily fished ecosystem. *Current Biology*, 16, 492–493.
https://doi.org/10.1016/j.cub.2006.06.018
Lynch, M. & Crease, T.J. (1990). The analysis of population survey data on DNA sequence variation. *Molecular Biology and Evolution*, 7, 377–394.
https://doi.org/10.1093/oxfordjournals.molbev.a040607
Maposa, S. (2005) Jellyfish plague hobbles Koeberg. Available from: https://www.iol.co.za/news/south-africa/jellyfish-plague-hobbles-koeberg-240851 (accessed 21 September 2015)
Mariottini, G.L., Giacco, E. & Pane, L. (2008) The mauve stinger *Pelagia noctiluca* (Forsskal, 1775). Distribution, ecology, toxicity and epidemiology of stings. A review. *Marine Drugs*, 6, 496–513.

https://doi.org/10.3390/md20080025
Mariscal, R.N. (1974) Nematocysts. *In*: Muscatine, L. & Lenhoff, H.M. (Eds.), *Coelenterate biology: reviews and new perspectives*. Academic Press, New York, pp. 129–178.
https://doi.org/10.1016/B978-0-12-512150-7.50008-6
Mayer, A.G. (1910) Volume III: Schyphomedusae. *In*: *Mayer, A.G., Medusae of the world*. Carnegie Institute, Washington, pp. 499–735.
https://doi.org/10.5962/bhl.title.159245
McClain, C.R., Balk, M.A., Benfield, M.C., Branch, T.A., Chen, C., Cosgrove, J., Dove, A.D.M., Gaskins, L.C., Helm, R.R., Hochberg, F.G., Lee, F.B., Marshall, A., McMurray, S.E., Schanche, C., Stone, S.N. & Thaler, A.D. (2015) Sizing ocean giants: patterns of intraspecific size variation in marine megafauna. *PeerJ*, 3, e715
https://doi.org/10.7717/peerj.715
Medlin, L.K., Elwood, H.J., Stickel, S. & Sogin, M.L. (1988) The characterization of enzymatically amplified eukaryotic 16S-like rRNA-coding regions. *Gene*, 71, 491–499.
https://doi.org/10.1016/0378-1119(88)90066-2
Mejía-Sánchez, N. & Marques, A.C. (2013) Getting information from ethanol preserved nematocysts of the venomous cubomedusa Chiropsalmus quadrumanus: a simple technique to facilitate the study of nematocysts. *Latin American Journal of Aquatic Research*, 41 (1), 166–169.
https://doi.org/103856/vol41-issue1-fulltext-14
Mello, B. (2018) Estimating TimeTrees with MEGA and the TimeTree Resource. *Molecular Biology and Evolution*, 35 (9), 2334–2342
https://doi.org/10.1093/molbev/msy133
Mianzan, H.W. & Cornelius, P.F.S. (1999) Cubomedusae and Scyphomedusae. *In*: Boltovskoy, D. (Ed.), *South Atlantic Zooplankton. Vol. 1*. Backhuys Publishers, Leiden, pp. 513–559.
Miller, G.A. & Chapman, J.P. (2001) Misunderstanding analysis of covariance. *Journal of Abnormal Psychology*, 110 (1), 40–48.
https://doi.org/10.1037/0021-843X.110.1.40
Mills, C.E. (2001) Jellyfish blooms: are populations increasing globally in response to ocean conditions? *Hydrobiologia*, 451, 55–68.
https://doi.org/10.1007/978-94-010-0722-1_6
Morandini, A.C. & Marques, A.C. (2010) Revision of the genus *Chrysaora* Péron & Lesuer, 1810 (Cnidaria: Scyphozoa). *Zootaxa*, 2464 (1), 1–97.
https://doi.org/10.11646/zootaxa.2464.1.1
Neethling, S. (2010) *Re-descriptions of some South African scyphozoa: out with the old and in with the new*. MSc thesis University of the Western Cape, University of the Western Cape, 172 pp. [unpublished notes]
Nei, M. (1987) *Molecular Evolutionary Genetics*. Columbia University Press, New York, 512 pp.
https://doi.org/10.7312/nei-92038
Nei, M. & Kumar, S. (2000) *Molecular Evolution and Phylogenetics*. Oxford University Press, New York, 333 pp.
Nylander, J.A.A. (2004) *MrModeltest. Version 2*. Program Distributed by the Author. Evolutionary Biology Centre, Uppsala University, Uppsala, Sweden. [software]
Ogden, T. & Rosenberg, M. (2007) How should gaps be treated in parsimony? A comparison of approaches using simulation. *Molecular phylogenetics and evolution*, 42, 817–826.
https://10.1016/j.ympev.2006.07.021
Östman, C. (2000) A guideline to nematocyst nomenclature and classification, and some notes on the systematic value of nematocysts. *Scientia Marina*, 64 (1), 31–46.
https://doi.org/10.3989/scimar.2000.64s131
Pagès, F., Gili, J.M. & Bouillon, J. (1992) Medusae (Hydrozoa, Scyphozoa, Cubozoa) of the Benguela Current (southeastern Atlantic). *In*: Pagès, F., Gili, J.M. & Bouillon, J. (Eds.), Planktonic Cnidarians of the Benguela Current. *Scientia Marina*, 56 (Supplement 1), pp. 1–64.
Palomares, M.L.D. & Pauly, D. (2009) The growth of jellyfishes. *Hydrobiologia*, 616, 11–21.
https://doi.org/10.1007/s10750-008-9582-y
Papenfuss, E.J. (1936) The utility of the nematocysts in the classification of certain Scyphomedusae. I. *Cyanea capillata*, *Cyanea palmstruchii*, *Dactylometra quinquecirrha*, *Dactylometra quinquecirrha* var. *chesapeakei*, and *Chrysaora hysoscella*. *Acta Universitatis Lundensis*, Nova Series, 31 (11), 19–26.
Peach, M.B. & Pitt, K.A. (2005) Morphology of the nematocysts of the medusae of two scyphozoans, *Catostylus mosaicus* and *Phyllorhzia punctata* (Rhizostomeae): implications for capture of prey. *Invertebrate biology*, 124 (2), 98–108.
https://doi.org/10.1111/j.1744-7410.2005.00012.x
Péron, F. & Lesueur, C.A. (1810) Tableau des caractères génériques et spécifiques de toutes les espèces de Méduses connues jusqu‟à ce jour. *Annales du Muséum National d'Histoire Naturelle, Paris*, 14, 325–366.
Purcell, J.E., Uye, S. & Lo, W. (2007) Anthropogenic causes of jellyfish blooms and their direct consequences for humans: a review. *Marine Ecology Progress Series*, 350, 153–174.
https://doi.org/10.3354/meps07093

Quinn, G. & Keough, M. (2002) *Experimental Design and Data Analysis for Biologists*. Cambridge University Press, Cambridge, 537 pp.
https://doi.org/10.1017/cbo9780511806384
Ramhaut, A. (2009) FigTree. Version 1.4.1 Available from: http://tree.bio.ed.ac.uk/software/figtree/ (accessed 8 May 2013)
Ramhaut, A. & Drummond, A.J. (2007) Tracer. Version 1.5. Available from: http://beast.bio.ed.ac.uk/Tracer/ (accessed 8 May 2013)
Ranson, G. (1949) Résultats scientifiques des croisières du navire école belge "Mercator" IV. II Méduses. *Mémoires du Institut Royal des Sciences Naturelles de Belgique*, Série 2, 33, 121–158.
Reynaud, A.A.M. (1830) Medusa (Cyanea) *caliparea*; Medusa (Rhyzostoma) *fulgida*. *In*: Lesson, R.P. (Ed.), *Centurie Zoologique, ou choix d'animaux rares, nouveaux ou imparfaitement connus*. F.G. Levrault, Paris, pp. 67–68, 79–80.
Ronquist, F. & Huelsenbeck, J.P. (2003) MrBayes 3: Bayesian phylogenetic inference under mixed models. *Bioinformatics*, 19, 1572–1574.
https://doi.org/10.1093/bioinformatics/btg180
Sambrook, J. & Russell, D.W. (2001) *Molecular Cloning: A Laboratory Manual*. Cold Spring Harbor Laboratory Press, Cold Spring Harbor, New York, 34 pp.
Sink, K.J., Gibbons, M.J., Laird, M.C. & Atkinson, L.J. (2017) Phylum Cnidaria *In*: Atkinson, L.J. & Sink, K.J. (Eds.), *Field Guide to the Offshore Marine Invertebrates of South Africa*, Malachite Marketing and Media, Pretoria, pp. 65–115.
Sparks, C., Buecher, E., Brierley, A.S., Boyer, H., Axelsen, B.E. & Gibbons, M.J. (2001) Observations on the distribution and relative abundance of the scyphomedusan *Chrysaora hysoscella* (Linné, 1766) and the hydrozoan *Aequorea aequorea* (Forskål, 1775) in the northern Benguela ecosystem. *Hydrobiologia*, 451, 275–286.
https://doi.org/10.1023/A:1011829516239
Stiasny, G. (1934) Die rhizostomeen-sammlung des British Museum (Natural History) in London. *Zoologische Mededeelingen*, 14, 137–178.
Stiasny, G. (1939) Über *Dactylometra fulgida* (Reynaud) von der Walfischbai. *Zoologischer Anzeiger*, 126, 172–185.
Straehler-Pohl, I. & Jarms, G. (2010) Identification key for young ephyrae: a first step for early detection of jellyfish blooms. *Hydrobiologia*, 645, 3–21.
https://doi.org/10.1007/s10750-010-0226-7
Suchman, C.L., Daly, E.A., Keister, J.E., Peterson, W.T. & Brodeur, R.D. (2008) Feeding patterns and predation potential of scyphomedusae in a highly productive upwelling region. *Marine Ecology Progress Series*, 358, 161–172.
https://doi.org/10.3354/meps07313
Swofford, D. (2003) *PAUP—Phylogenetic Analysis Using Parsimony (* and Other Methods). Version 4.0b10*. Sinauer Associates, Sunderland, Massachusetts. [software]
Tajima, F. (1983) Evolutionary relationship of DNA sequences in finite populations. *Genetics*, 105, 437–460.
Tamura, K., Battistuzzi. F.U., Billing-Ross, P., Murillo, O., Filipski, A. & Kumar, S. (2012) Estimating Divergence Times in Large Molecular Phylogenies. *Proceedings of the National Academy of Sciences*, 109, 19333–19338.
https://doi.org/10.1073/pnas.1213199109
Thiel, H. (1966) The evolution of the Scyphozoa, a review. *In*: Rees, W.J. (Ed.), *Cnidaria and their Evolution*. Academic Press, London, pp. 77–117.
Thibault-Botha, D. & Bowen, T. (2004) Impact of formalin preservation on *Pleurobrachia bachei* (Ctenophora). *Journal of Experimental Marine Biology and Ecology*, 303, 11–17.
https://doi.org/10.1016/j.jembe.2003.10.017
van der Lingen, C.D., Shannon, L.J., Cury, P., Kreiner, A., Moloney, C.L., Roux, J.-P. & Vaz- Velho, F. (2006) Resource and Ecosystem Variability, Including Regime Shifts, in the Benguela Current System. *In:* Shannon, V., Hempel, G., Malanotte-Rizzoli, P., Moloney, C. & Woods, J. (Eds.), *Large Marine Ecosystems. Vol. 14*. Elsevier, pp. 146–184.
https://doi.org/10.1016/s1570-0461(06)80013-3
Vanhöffen, E. (1888) Untersuchungen über semäostome und rhizostome Medusen. *Bibliotheca Zoologica*, 1, 5–52.
https://doi.org/10.5962/bhl.title.38091
Vanhöffen, E. (1902) Die Acraspeden Medusen der deutschen Tiefsee-expedition 1898–1899. *Wissenschaftliche Ergebnisse der deutschen Tiefsee-expedition auf dem dampfer Valdivia 1898–1899*, 3, 3–52.
https://doi.org/10.5962/bhl.title.1404
Venter, G.E. (1988) Occurrence of jellyfish on the west coast off south west Africa/Namibia, in Long-term data series relating to southern Africa's renewable natural resources. *South African National Science Progress Reports*, 157, 56–61.
Vousden, D., Stapley, J.R., Ngoile, M.A.K., Sauer, W. & Scott, L. (2012) Climate change and variability of the Agulhas and Somali Current Large Marine Ecosystem in relation to socioeconomics and governance. Chapter 5 in: *Frontline observations on climate change and sustainability of Large Marine Ecosystems*, 17, 81–96.
Wallace, D.M. (1987) Large- and small-scale phenol extractions. *Methods in Enzymology*, 152, 33–41.
https://doi.org/10.1016/0076-6879(87)52007-9
Widmer, C.L. (2005) Effects of temperature on growth of north-east Pacific moon jellyfish ephyrae, *Aurelia labiata* (Cnidaria: Scyphozoa). *Journal of the Marine Biological Association of the United Kingdom*, 85, 569–573.
https://doi.org/10.1017/S0025315405011495
Zar, J.H. (1999) *Biostatistical Analysis. 4th Edition*. Dorling Kindersley, New Delhi, 663 pp.

APPENDIX 1. Table showing the locality information for specimens of *Chrysaora agulhensis* **sp. nov.**, *C. fulgida* and *C. africana* used in the genetic analyses of this study (refer to Figs 2–3). Corresponding GenBank accession numbers for the COI, 18S and ITS gene regions are also shown.

Specimen number	Species	Location	COI	18S	ITS
C3	*C. agulhensis* **sp. nov.**	34.13˚S, 18.44˚E	MT235601	-	-
F44	*C. agulhensis* **sp. nov.**	34.10˚S, 18.48˚E	MT235588	MT235578	MT235560
F1	*C. agulhensis* **sp. nov.**	33.81˚S, 18.39˚E	MT235591	MT235579	MT235561
V11	*C. agulhensis* **sp. nov.**	34.10˚S, 18.49˚E	MT235585	MT235576	MT235557
M10	*C. agulhensis* **sp. nov.**	34.11˚S, 18.37˚E	MT235586	MT235577	MT235559
G1	*C. agulhensis* **sp. nov.**	33.87°S, 18.30°E	MT235587	-	-
XW	*C. agulhensis* **sp. nov.**	33.87°S, 18.30°E	-	MT235575	MT235558
CF06	*C. fulgida*	34.82°S, 19.65°E	MT235597	MT235571	MT235567
CFE1	*C. fulgida*	22.93°S, 14.51°E	MT235594	MT235582	MT235564
CFE2	*C. fulgida*	22.93°S, 14.51°E	MT235593	MT235581	MT235563
F8	*C. fulgida*	34.10˚S, 18.48˚E	MT235589	-	-
F1B	*C. fulgida*	34.98°S, 19.79°E	MT235590	-	-
CFL1	*C. fulgida*	34.11˚S, 18.37˚E	MT235592	MT235580	MT235562
CF20	*C. fulgida*	23.67˚S, 13.25˚E	MT235596	MT235584	MT235566
CF45	*C. fulgida*	34.82°S, 19.65°E	MT235595	MT235583	MT235565
CA21	*C. africana*	34.10˚S, 18.48˚E	MT235599	MT235573	MT235569
CA3	*C. africana*	22.95°S, 14.48°E	MT235600	MT235574	MT235570
CAE	*C. africana*	22.93°S, 14.47°E	MT235598	MT235572	MT235568

APPENDIX 2: Relative abundance of various nematocysts occurring within the tentacles and oral arms of *Chrysaora agulhensis* **sp. nov.**, *Chrysaora fulgida* and *Chrysaora africana*. Table also indicates Simpson's diversity index (D) as well as Simpson's reciprocal index (1/D).

Species/Tissue	Holotrichous O-isorhiza	Heterotrichous microbasic bi-rhopaloid	Holotrichous A-isorhiza	Heterotrichous microbasic eurytele	Atrichous isorhiza	D^	1/D^
***C. agulhensis* sp. nov. oral arm**	62	174	3	12	0	0.26	3.88
***C. agulhensis* sp. nov. tentacles**	112	343	2	0	5	0.30	3.37
***C. africana* oral arm**	101	262	0	0	4	0.34	2.94
***C. africana* tentacles**	94	269	0	0	0	0.28	3.54
***C. fulgida* oral arm**	61	132	17	0	1	0.33	3.07
***C. fulgida* tentacles**	232	170	92	0	0	0.29	3.42

APPENDIX 3: Mean measures of various features of the rhopalia, ephyrae and polyps of *Chrysaora agulhensis* **sp. nov.**, *C. fulgida* and *C. africana*. Measures represented as mean ± standard error.

Rhopalia			
	C. agulhensis **sp. nov.**	*C. fulgida*	*C. africana*
Length of rhopalar canal (mm)	5.1 ± 1.2	5.7 ± 2.2	6 ± 2.5
Length of hood (mm)	5.5 ± 2.3	1.5 ± 0.22	2.3 ± 0.9
Length of statocyst (mm)	2.2 ± 0.8	2.75 ± 1.1	1.78 ± 0.6
Length of basal stem (mm)	2.45 ± 0.9	3.2 ± 1.1	4.76 ± 1.8
Ephyrae			
No. of lappet stems	8	8	
No. of lappets	16	16	
Lappet length (mm)	0.4 ± 0.1	0.3 ± 0.1	
Stem length (mm)	0.85 ± 0.2	0.6 ± 0.2	
Manubrium length (mm)	0.48 ± 0.5	0.7 ± 0.2	
Mouth diameter (mm)	0.63 ± 0.3	0.38 ± 0.1	
Length of rhopalar canal (mm)	0.38 ± 0.1	0.33 ± 0.2	
Oral disk diameter (mm)	0.75 ± 0.3	0.93 ± 0.2	
Diameter of ephyrae (mm)	2.35 ± 0.6	2.1 ± 0.4	
Polyp			
Overall height (mm)	3.5 ± 1.2	4.3 ± 1.6	
Diameter of oral disk (mm)	1.82 ± 0.9	2.5 ± 1.1	
No. of tentacles (mm)	16	16	
Tentacle length (mm)	16.23 ± 5.3	15.83 ± 4.8	